Molecular Vision 2019; 25:869-889 <http://www.molvis.org/molvis/v25/869>
Received 6 April 2019 | Accepted 28 December 2019 | Published 30 December 2019

Sector retinitis pigmentosa: Report of ten cases and a review of the literature

Razek Georges Coussa,[1] Diana Basali,[1] Akiko Maeda,[2] Meghan DeBenedictis,[1] Elias I. Traboulsi[1]

(The first two authors contributed equally to this study.)

[1]Center for Genetic Eye Diseases, Cole Eye Institute, Cleveland Clinic, Cleveland, OH; [2]Department of Ophthalmology & Visual Sciences, Case Western Reserve University School of Medicine, Cleveland, OH.

Purpose: To describe the genotypes and phenotypes of ten patients with sector retinitis pigmentosa (RP). We also review previously reported mutations associated with sector RP and provide a discussion of possible underlying pathophysiological mechanisms.

Methods: Patients underwent detailed ophthalmologic examinations, fundus photography, fundus autofluorescence (FAF) imaging, spectral-domain optical coherence tomography (SD-OCT), as well as visual field and electroretinographic testing. All patients underwent genetic testing to identify the molecular etiology of their disease.

Results: A total of ten patients were studied. Among these patients, nine had mutations in *RHO* (c.677T>C; p.Leu226Pro (novel), c.68C>A; p.Pro23His, c.808A>C; p.Ser270Arg, c.44A>G; p.Asn15Ser, and c.325G>A; p.Gly109Arg), and one patient had a mutation in *RPGR* (c.3092_3093delAG; p.Glu1031Glyfs*47). All patients with missense mutations in *RHO* had visual acuities (VAs) better than 20/30 and showed a retained foveal ellipsoid zone and overlying retinal structures. The patient with the c.3092_3093delAG deletion in *RPGR* had VA of 20/60 oculus dexter (OD) and 20/400 oculus sinister (OS), as well as significant foveal thinning and contour atrophy. All patients showed pigmentary changes, or marked atrophy along the inferior arcades, or both. This pattern of degeneration corresponded to hypo- and hyperFAF and superior visual defects.

Conclusions: Sector RP is an uncommon form of RP in which only one or two retinal quadrants display clinical pathological signs. The great majority of cases result from mutations in *RHO.* The present data confirmed previously reported phenotypic manifestations of sector RP. Inferior retinal quadrants are possibly more severely affected due to greater light exposure.

Retinitis pigmentosa (RP) is genetically heterogeneous with causative mutations in more than 60 autosomal dominant, autosomal recessive, X-linked, and mitochondrial genes (RetNet) [1]. In general, the disease begins with rod photoreceptor degeneration followed by cone photoreceptor dysfunction; thus, patients develop night blindness and progressive peripheral constriction of the visual field followed by impairment of central and color vision [2]. The typical retinal phenotype is characterized by attenuated blood vessels, a pale optic nerve, and panretinal peripheral fundal changes characterized predominantly by the formation of bone spicules and variable atrophy. Retinal degeneration with clinical features of RP may also occur as part of systemic disorders, such as Usher syndrome, Bardet-Biedl syndrome, and others [1].

Sector RP designates an atypical form of RP in which only one or two fundus quadrants show clinical signs of the disease [3]. It is usually bilateral and symmetrical, and involves the inferior quadrants. However, there have been cases of unilateral or asymmetrical involvement, as well as ones in which degeneration of the nasal, superotemporal, or superior quadrants occurs [3]. Slow clinical progression, regionalized areas of bone spicule-like pigmentation, subnormal electroretinographic (ERG) amplitudes, and visual field defects corresponding to the affected retinal quadrants are all characteristics of sector RP. In the literature to date, sector RP has been reported to result from mutations in the rhodopsin (*RHO*, 3q22.1, OMIM 180380), usherin (*USH1C*, 11p15.1, OMIM 605242), and cadherin 23 (*CDH23*, 10q22.1, OMIM 605516) genes (Table 1).

We describe the genotypes and phenotypes of ten patients with sector RP, including a mother and son with a novel mutation in *RHO.* We also provide a review of previously reported mutations associated with sector RP, and a discussion of possible underlying molecular pathophysiological mechanisms.

Correspondence to: Elias I. Traboulsi, i32, 9500 Euclid Avenue, Cleveland, OH, 44195; Phone: (216)-444-2030, FAX: (216)-444-2226; email traboue@ccf.org

METHODS

Written informed consent was obtained from all patients after explaining the nature and possible consequences of the study. All study procedures conformed to the tenets of the Health Insurance Portability and Accountability Act and the Declaration of Helsinki for research involving human participants.

Ophthalmic examination: The patients were evaluated in a specialized retinal dystrophy clinic. Family and medical histories were obtained. Fundus photography, Goldmann visual field testing, fundus autofluorescence (FAF) imaging, and spectral-domain optical coherence tomography (SD-OCT) were performed. The diagnosis of sector RP was based on the presence of characteristic RP fundus features in one or two retinal quadrants and sparing of other quadrants.

Gene sequencing: Of the ten patients in this case series, seven had full sequence analysis of the *RHO* gene through a Clinical Laboratory Improvement Amendments (CLIA) certified laboratory. Patient 5 was the sister of patient 4 and had targeted mutation analysis for the mutation previously identified in her sibling. Given the clinical presentation and history, X-linked RP was suspected in patient 10, and he had genetic testing via sequence analysis of only the RP GTPase Regulator gene (*RPGR*, Xp11.4, OMIM 312610) gene.

Literature search: A comprehensive literature search was performed using PubMed and Scopus. The key phrase "sector retinitis pigmentosa" was used in both search engines, and all articles were explored for reported genetic mutations leading to sector RP. The references listed in papers found using Scopus and PubMed were also searched to ensure that all published papers containing gene mutations associated with sector RP were included in Table 1. Biochemical properties of mutations in the rhodopsin gene that cause sector RP were researched and are summarized in the Results section.

Table 1. Previous reported mutations causing sector RP.

Gene	Protein variation	Zygosity
RHO	p.Asn15Ser [77]	Heterozygous
	p.Thr17Met [66,78]	Heterozygous
	p.Pro23His [79]	Heterozygous
	p.Thr4Lys [80]	Heterozygous
	p.Thr58Arg [81]	Heterozygous
	p.Thr58Met [3]	Heterozygous
	p.Asn78Ile [82]	Heterozygous
	p.Gly106Arg [83]	Heterozygous
	p.Pro170His [84]	Heterozygous
	p.Gly182Ser [66]	-
	p.Asp190Asn [85]	Heterozygous
	p.Pro267Arg [86]	-
	p.Trp126Leu [87]	Heterozygous
	p.Asn15Ser [88]	Heterozygous
	p.Gly106Arg [89]	Heterozygous
CDH23	p.Pro2844Thr [51]	Heterozygous
USH1C	p.Arg103His [90]	Heterozygous

RESULTS

Clinical phenotypes and molecular diagnosis in sector RP cases: Patient 1 presented with nyctalopia and carries a c.68C>A;p.Pro23His mutation in *RHO.* He has visual field defects in the superior quadrants, corresponding to pigmentary changes and the hyper- and hypo-AF pattern in the inferior part of the retina (Figure 1, Appendix 1). Patient 2 has a c.677T>C;p.Leu226Pro novel mutation in *RHO,* a novel mutation in *RHO*, and shows superior visual field loss (Figure 2, Appendix 1). Patient 3 is the biological son of patient 2 and harbors the same c.677T>C;p.Leu226Pro novel mutation in *RHO* (Figure 3, Appendix 1). The siblings, patients 4 and 5, have a c.808A>C;p.Ser270Arg mutation in *RHO.* Their examinations revealed atrophic pigmentary RPE changes and a noticeable hyper- and hypo-AF pattern in the inferior retina, corresponding to the super visual field defects in both eyes (OU; Figure 4 and Figure 5, Appendix 1). Patient 6, who carries a c.44A>G;p.Asn15Ser mutation in *RHO*, has severe inferior chorioretinal atrophic changes associated with bone spicules and circumferential constriction of his visual fields (Figure 6, Appendix 1). Patient 7 has a c.44A>G;p.Asn15Ser mutation in *RHO* and demonstrated pigmentary changes along the inferior arcades that correlate with mild superior visual field defects. Interestingly, patient 7's OCT showed marked retinal layer contour abnormalities and thinning as well as RPE hyper-reflective round deposits in both eyes (Figure 7, Appendix 1). Patient 8 with a c.325G>A;p.Gly109Arg mutation in *RHO* has attenuation of inferior arterioles with perivascular hyperpigmentation, RPE atrophy, and pigmentary changes mainly in the inferior and inferonasal midperiphery. These findings corresponded to the patient's superonasal visual field defects (Figure 8, Appendix 1). Patient 9 has a c.68C>A; p.Pro23His mutation in *RHO* and inferotemporal bone spicules with corresponding significant superior and nasal constriction of his visual fields (Figure 9, Appendix 1). Patient 10 with a c.3092_3093delAG; p.Glu1031Glyfs*47 in *RPGR* showed circumferential constriction with superior VF defects and prominent RPE changes in the inferonasal quadrants. Of note is that the patient's OCT was significant for generalized foveal thinning with marked ellipsoid zone abnormalities, as well as RPE hyper-reflective round deposits

and diffuse thickening of the RPE band (Figure 10, Appendix 1).

Biochemistry and animal studies for rhodopsin mutations that cause sector RP: Several missense mutations of rhodopsin have been reported to cause sector RP, including the ones in this study (Figure 11). Among them, the proline to histidine mutation in codon 23 (p.Pro23His) is frequently reported, and accounts for about 12–14% of Americans of European origin [4]. The p.Pro23His mutation is located on the extracellular N-terminal tail region of rhodopsin. The p.Asn15Ser and p.Thr17Met mutations are also located in the same tail region. Biochemical properties of the rhodopsin p.Pro23His, p.Asn15Ser, and p.Thr17Met mutations have been well characterized. Several animal models have been studied in *RHO*-induced retinal degeneration, including Pro23 [5-8], Thr17 [9], Thr4 [10], and Asp190 [11]. In the following sections, we review the effect of reported mutations in rhodopsin on the function of the protein in animal models and in the laboratory.

p.Pro23His found in this study: The p.Pro23His mutation has been well studied, because it is the most common cause of autosomal dominant RP (adRP) in North America [12] and the first identified mutation for RP [13]. The first transgenic mouse models were established in 1992 [14], and rat p.Pro23His models are also available [15,16]. A swine p.Pro23His model was also established [17]. A knock-in (KI) mouse model of p.Pro23His that resembles the human condition more faithfully was created and characterized by Sakami et al. [18,19]. The homozygous mouse displays severe and rapidly progressive retinal degeneration, and the majority of rod photoreceptor cells are not visible by the age of 2 months. The heterozygous p.Pro23His KI mouse shows milder retinal degeneration with predominant involvement of the inferior retina, and rod photoreceptor cells are still observed at the age of 4 months. Partial rescue of the rod photoreceptor cells was induced by genetic deletion of visual chromophore 11-*cis*-retinal by crossing with the Lecithin:retinol acyltransferase (*Lrat*) knockout mouse [20], suggesting structural instability of rhodopsin with p.Pro23His. Glycosylation of rhodopsin was also impaired in p.Pro23His KI mouse retinas. Accumulation of p.Pro23His rhodopsin in the endoplasmic reticulum (ER) of the inner segments was not observed with immunohistochemistry in the p.Pro23His KI mouse, in contrast to studies with a mouse model with the mutations p.Val20Gly, p.Pro23His, and p.Pro27Leu (namely, a VPP mouse model) and transgenic *Xenopus laevis* expressing p.Pro23His in their photoreceptors that provided evidence of ER stresses by mutant rhodopsin [21,22]. Light-induced photoreceptor degeneration and acceleration of the speed of photoreceptor degeneration under vitamin A depletion have been also reported in the *Xenopus laevis* model of p.Pro23His [23]. Additionally, the rate of photoreceptor degeneration in dark-reared transgenic mice was significantly slower than in transgenic mice raised under cyclic light conditions [6]. p.Pro23His expressed in *Caenorhabditis elegans* aggregates in the nervous system, but the pharmacological chaperone 9-*cis*-retinal stabilizes it during biogenesis [24]. In vitro, p.Pro23His binds to 9-*cis*-retinal to produce isorhodopsin, and it is folded correctly with formation of the appropriate disulfide bond. In *C. elegans* neurons, p.Pro23His isorhodopsin initiates phototransduction by coupling with the endogenous Gi/o G-protein signaling cascade that induces loss of locomotion. However, regeneration of p.Pro23His isorhodopsin with 9-*cis*-retinal chromophore is slower than that of wild type isorhodopsin, suggesting that combined with the inherent instability of p.Pro23His rhodopsin, this could lead to the structural cellular changes and photoreceptor death. The p.Pro23His protein expressed in HEK293S cells showed decreased protein stability, decreased photobleaching spectra, mislocalization in the ER, and abnormal glycosylation [25].

p.Leu226Pro found in this study: Leu226 is located in helix 5 of rhodopsin. Leu226 is a key hydrophobic patch in rhodopsin that can bind with transducin, the cognate G-protein of rhodopsin [26]. Six residues of rhodopsin have been identified as transducin-binding sites, and Leu226 is the only residue in a rhodopsin helix. Leu226 also plays important roles with Thr229 and Val230 for helix 6 movement [27] and helix 3 [28].

p.Ser270Arg (p.Pro267Arg) found in this study: No studies on biochemical properties of the Ser270 residue have been reported to date, to the best of our knowledge, but the p.Pro267Arg mutation in rhodopsin has been examined. Ser270 and Pro267 are located in helix 6, which swings off the cytoplasmic side of the helix between at Meta I and Meta II states in the process of rhodopsin activation [29]. Cys264 and Trp265 contribute to make a groove for visual chromophore binding at Lys296 in helix 7. p.Pro267Arg and p.Pro267Leu rhodopsin show abnormal bleaching behavior, misfolding, and mislocalization in the ER, as well as accelerated Meta II decay [30,31]. Lesser effects of Ser270 on Meta II decay and bleaching behavior are anticipated due to its increased distance from the chromophore-binding site compared to Pro267. Pro267 mutations have been reported in adRP [32].

T4K, T4L, N15S, and T17M: The N-X-S/T sequence is essential for N-linked protein glycosylation, and rhodopsin has two glycosylated asparagines (Asn) at the N-terminal tail at codon 2 and codon 15. N-linked glycosylation is a post-translational modification of proteins and participates

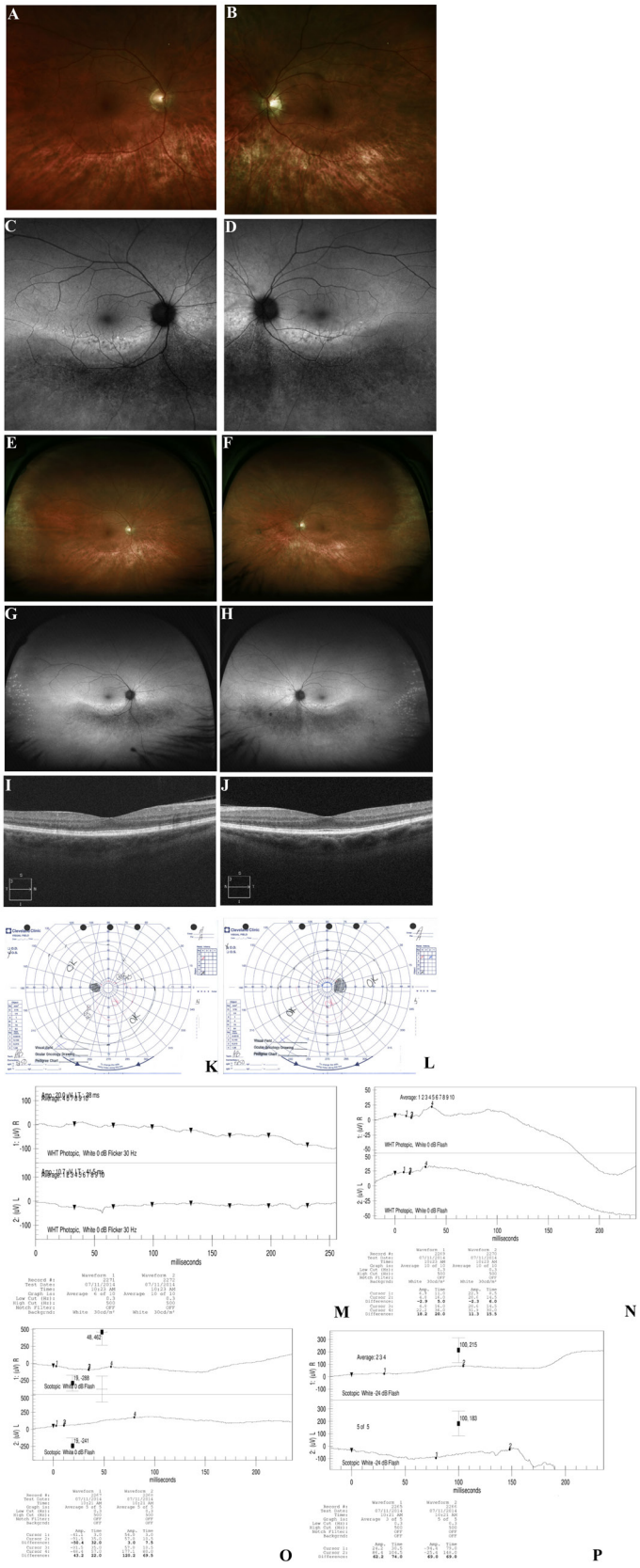

Figure 1. Clinical imagining of patient 1 with a c.68C>A mutation in *RHO* (Pro23His). **A**: Oculus dexter (OD) color photo of the posterior pole showing a normal exam. **B**: Oculus sinister (OS) color photo of the posterior pole showing a normal exam. **C**: OD fundus autofluorescence (FAF) photo of the posterior pole showing hyper-autofluorescence (hyperAF) most noticeable along the inferior arcade with adjacent hypoautofluorescence (hypoAF) with the speckled pattern of hyperAF outside the inferior arcade extending into the midperiphery. **D**: OS FAF photo of the posterior pole showing hyperAF most noticeable along the inferior arcade with adjacent hypoAF with the speckled pattern of hyperAF outside the inferior arcade extending into the midperiphery. **E**: OD widefield color fundus photo showing RPE hypopigmentation and atrophic changes most prominent along the inferior arcades midperipherally as well as in the temporal periphery. **F**: OS OD widefield color fundus photo showing RPE hypopigmentation and atrophic changes most prominent along the inferior arcades midperipherally as well as in the temporal periphery. **G**: OD widefield fundus FAF photo showing hyperAF most noticeable along the inferior arcade with adjacent hypoAF with the speckled pattern of hyperAF outside the inferior arcade extending into the midperiphery. **H**: OS widefield fundus FAF photo showing hyperAF most noticeable along the inferior arcade with adjacent hypoAF with the speckled pattern of hyperAF outside the inferior arcade extending into the midperiphery. **I**: OD foveal spectral-domain optical coherence tomography (SD-OCT) showing mild blunting of the foveal depression. **J**: OS foveal SD-OCT showing mild blunting of the foveal depression. **K**: OS Goldman visual field showing mild superior visual field loss. **L**: OD Goldman visual field showing mild superior visual field loss. **M**: OD photopic electroretinogram (ERG) response showing reduced low amplitudes. **N**: OS photopic ERG response showing reduced low amplitudes. **O**: OD scotopic ERG response showing reduced low amplitudes. **P**: OS scotopic ERG response showing reduced low amplitudes.

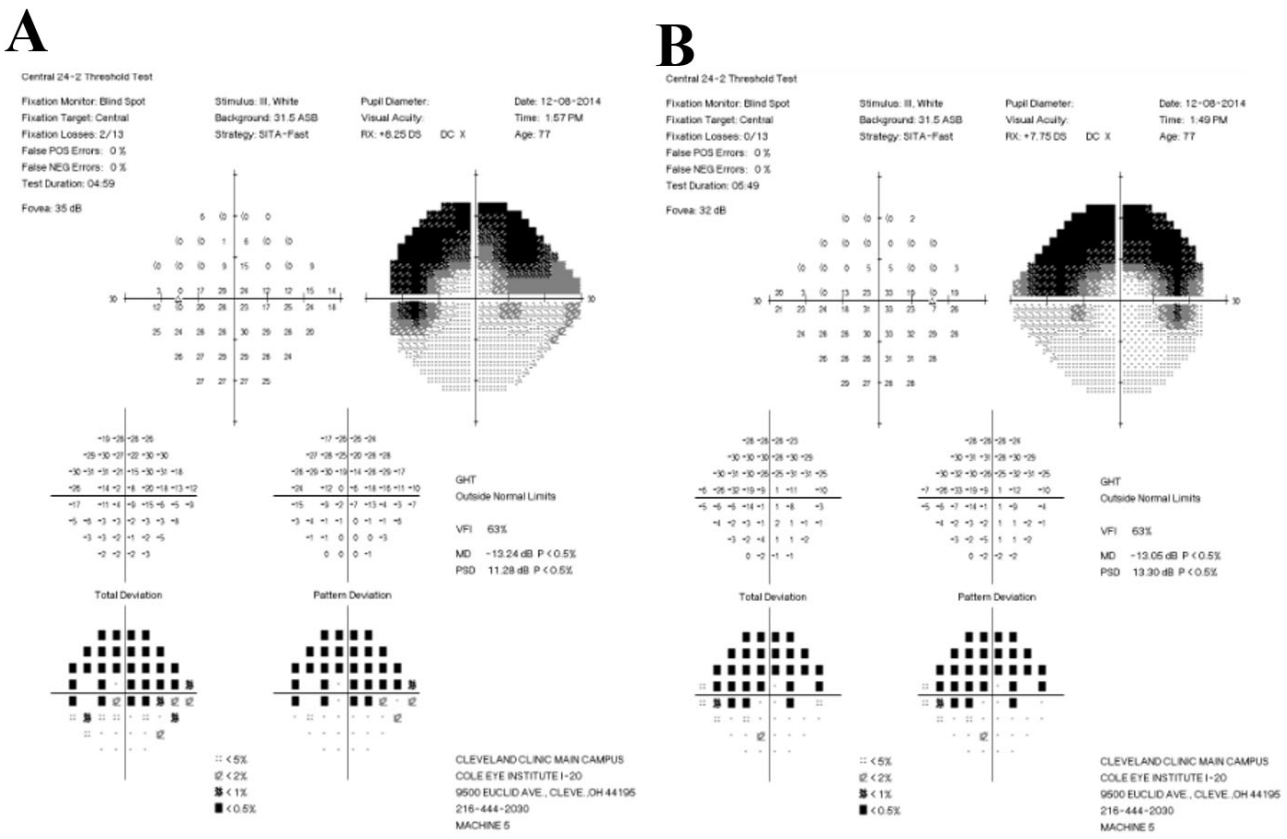

Figure 2. Visual field testing of patient 2 with a novel c.677T>C mutation in *RHO* (p.Leu226Pro). **A**: Oculus sinister (OS) Humphrey 24-2 SITA Fast visual field showing superior hemifield defects. **B**: Oculus dexter (OD) Humphrey 24-2 SITA Fast visual field showing superior hemifield defects.

in many important biological roles, such as protein folding, intracellular targeting, immune response, cell adhesion, and protease resistance. Asn15 is known to play more important roles than Asn2 in rhodopsin because Asn2 mutations have not been reported among glycosylation consensus sequences Asn2, Thr4, Asn15, and Thr17. p.Asn15Ser and p.Thr17Met mutations are associated with sector RP (Table 1). P.Thr17Met rhodopsin, which is expressed in HEK293S cells, showed low expression levels, accumulation in the ER, and less binding with visual chromophore 11-*cis*-retinal [25]. Reduced ability to activate the G-protein transducin has also been reported with p.Thr17Met rhodopsin, as well as non-glycosylated rhodopsin [32,33]. p.Asn15Ser and p.Thr17Met proteins expressed in *Xenopus laevis* cause photoreceptor degeneration [34]. Interestingly, these mutant proteins are less toxic in their dark inactive states, and light exposure exacerbates photoreceptor degeneration in the retina expressing these mutants. The p.Thr17Met protein expressed in the HEK293S cells showed decreased protein stability, decreased photobleaching spectra, mislocalization in the ER, and abnormal glycosylation [25]. A dog p.Thr4Arg model exhibited a distinct topographic pattern of retinal degeneration [35], and mislocalization of rhodopsin in the ER, aberrant glycosylation, and instability of rhodopsin were all observed [36].

p.Met39Arg: Met39 is located in helix 1 on one of the sites of the proposed retinal channel where the visual chromophore 11-*cis*-retinal can enter the protein, get isomerized, and exit upon Schiff's base breakage after the photoactivation cascade [37]. p.Met39Arg may alter the helix1–helix7 interface and the network of interactions between helices 1, 6, and 7, suggesting problems of receptor stability and the rate of Gt activation and retinal release [38]. p.Met39Arg showed a faster rate for transducing activation than WT rhodopsin with a faster metarhodopsin II decay [38].

p.Asn55Lys: Asn55 is part of the conserved GX3N motif in helix 1, which is conserved for allosteric interaction with transducin to initiate the phototransduction cascade [39,40]. p.Asn55Lys showed an altered retinal release from opsin binding pocket upon light exposure [38].

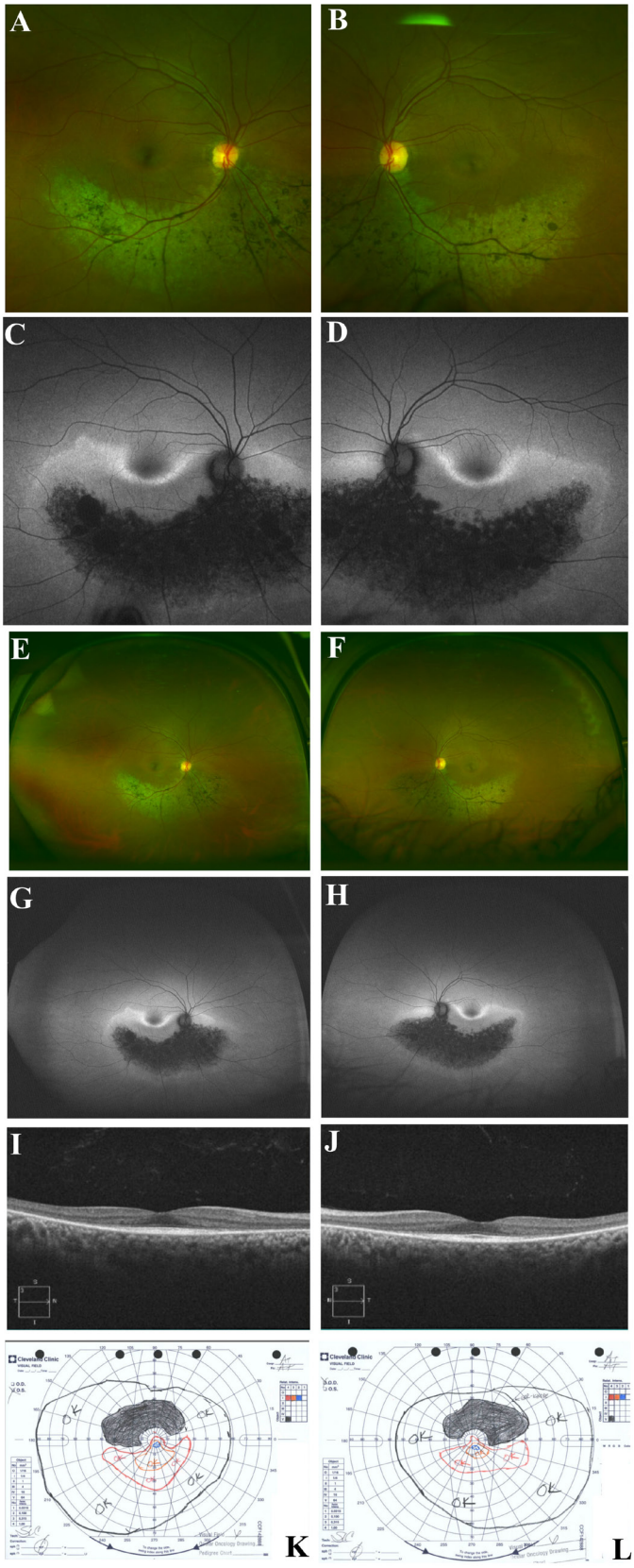

Figure 3. Clinical imagining of patient 3 with a novel c.677T>C mutation in *RHO* (p.Leu226Pro). **A**, **E**: Oculus dexter (OD) color photos showing RPE hypopigmentation and atrophic changes with bone spicules most prominent along the inferior arcades. **B**, **F**: Oculus sinister (OS) color photos showing RPE hypopigmentation and atrophic changes with bone spicules most prominent along the inferior arcades. **C**, **G**: OD fundus autofluorescence (FAF) photos showing crescent-shaped hyper-autofluorescence (hyperAF) contouring the fovea inferiorly and temporally as well as the optic nerve nasally. There is also a patchy pattern of hypoautofluorescence (hypoAF) along the inferior arcades just adjacent to the previously mentioned crescent-shaped hyperAF. **F**, **H**: OS FAF photos showing crescent-shaped hyperAF contouring the fovea inferiorly and temporally as well as the optic nerve nasally. There is also a patchy pattern of hypoAF along the inferior arcades just adjacent to the previously mentioned crescent-shaped hyperAF. **I**: OD foveal spectral-domain optical coherence tomography (SD-OCT) showing parafoveal retinal thinning and loss of the ellipsoid zone. **J**: OS foveal SD-OCT showing parafoveal retinal thinning and loss of the ellipsoid zone. **K**: OS Goldman visual field showing superior hemifield defects between the 10th and 30th degrees. **L**: OD Goldman visual field showing superior hemifield defects between the 10th and 30th degrees.

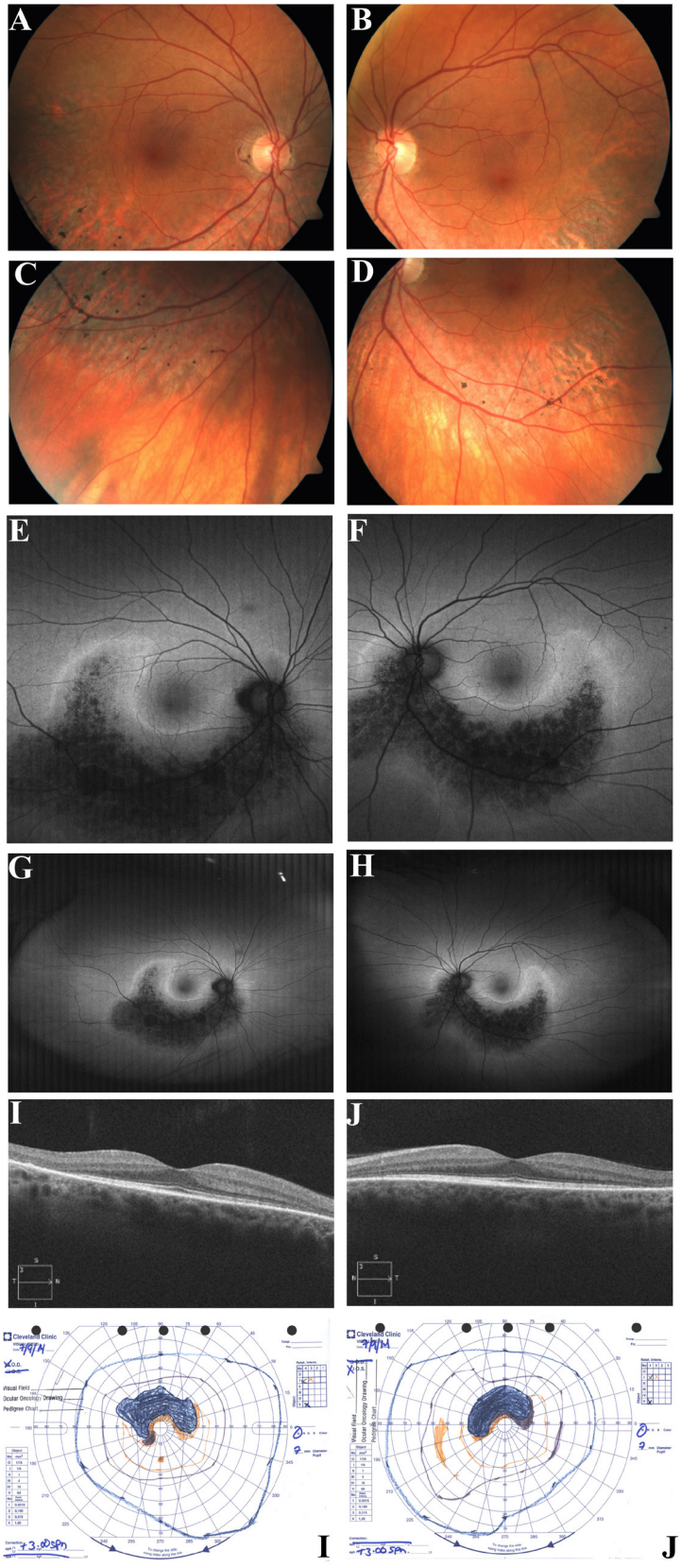

Figure 4. Clinical imagining of patient 4 with a c.808A>C mutation in *RHO* (p.Ser270Arg). **A**, **C**: Ocular dexter (OD) color photo of posterior pole showing RPE hypopigmentation and atrophic changes with occasional bone spicules most prominent along the inferior arcades. **B**, **D**: Oculus sinister (OS) color photo of posterior pole showing RPE hypopigmentation and atrophic changes with occasional bone spicules most prominent along the inferior arcades. **E**, **G**: OD fundus autofluorescence (FAF) photos showing crescent-shaped hyper-autofluorescence (hyperAF) contouring the fovea inferiorly and temporally as well as the optic nerve nasally. There is also a patchy pattern of hypoautofluorescence (hypoAF) along the inferior arcades just adjacent to the previously mentioned crescent-shaped hyperAF. **F**, **H**: OS FAF photos showing crescent-shaped hyperAF contouring the fovea inferiorly and temporally as well as the optic nerve nasally. There is also a patchy pattern of hypoAF along the inferior arcades just adjacent to the previously mentioned crescent-shaped hyperAF. **I**: OD foveal SD-OCT showing parafoveal retinal thinning and loss of the ellipsoid zone and photoreceptor layer most prominent in the inferior part of the posterior pole. **J**: OS foveal SD-OCT showing parafoveal retinal thinning and loss of the ellipsoid zone and photoreceptor layer most prominent in the inferior part of the posterior pole. **K**: OS Goldman visual field showing superior parafoveal arcuate-like scotoma within the central 40 degrees. **L**: OD Goldman visual field showing superior parafoveal arcuate-like scotoma within the central 40 degrees.

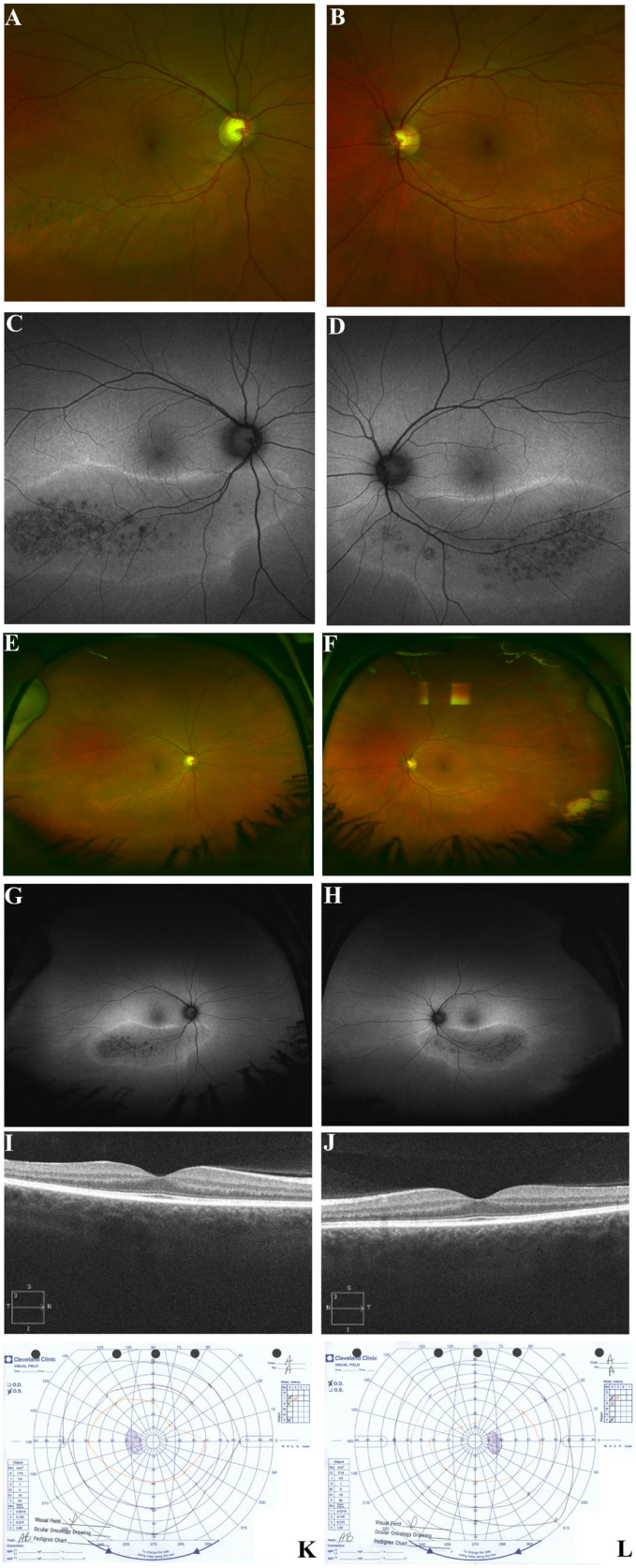

Figure 5. Clinical imagining of patient 5 with a c.808A>C mutation in *RHO* (p.Ser270Arg). **A**, **E**: Oculus dexter (OD) color photos showing an oval-shaped island of RPE hypopigmentation and atrophy extending from within the inferior posterior pole to the midperiphery and along the inferior arcades. **B**, **F**: Oculus sinister (OS) color photos showing an oval-shaped island of RPE hypopigmentation and atrophy extending from within the inferior posterior pole to the midperiphery and along the inferior arcades. **C**, **G**: OD fundus autofluorescence (FAF) photos showing an oval-shaped island of RPE hypopigmentation and atrophy extending from within the inferior posterior pole to the midperiphery and along the inferior arcades. **D**, **H**: OS FAF photos showing an oval-shaped island of RPE hypopigmentation and atrophy extending from within the inferior posterior pole to the midperiphery and along the inferior arcades. **I**: OD foveal spectral-domain optical coherence tomography (SD-OCT) showing normal retinal structures. **J**: OS foveal SD-OCT showing normal retinal structures. **K**: OS Goldman visual field showing mild superior visual field loss. **L**: OD Goldman visual field showing mild superior visual field loss.

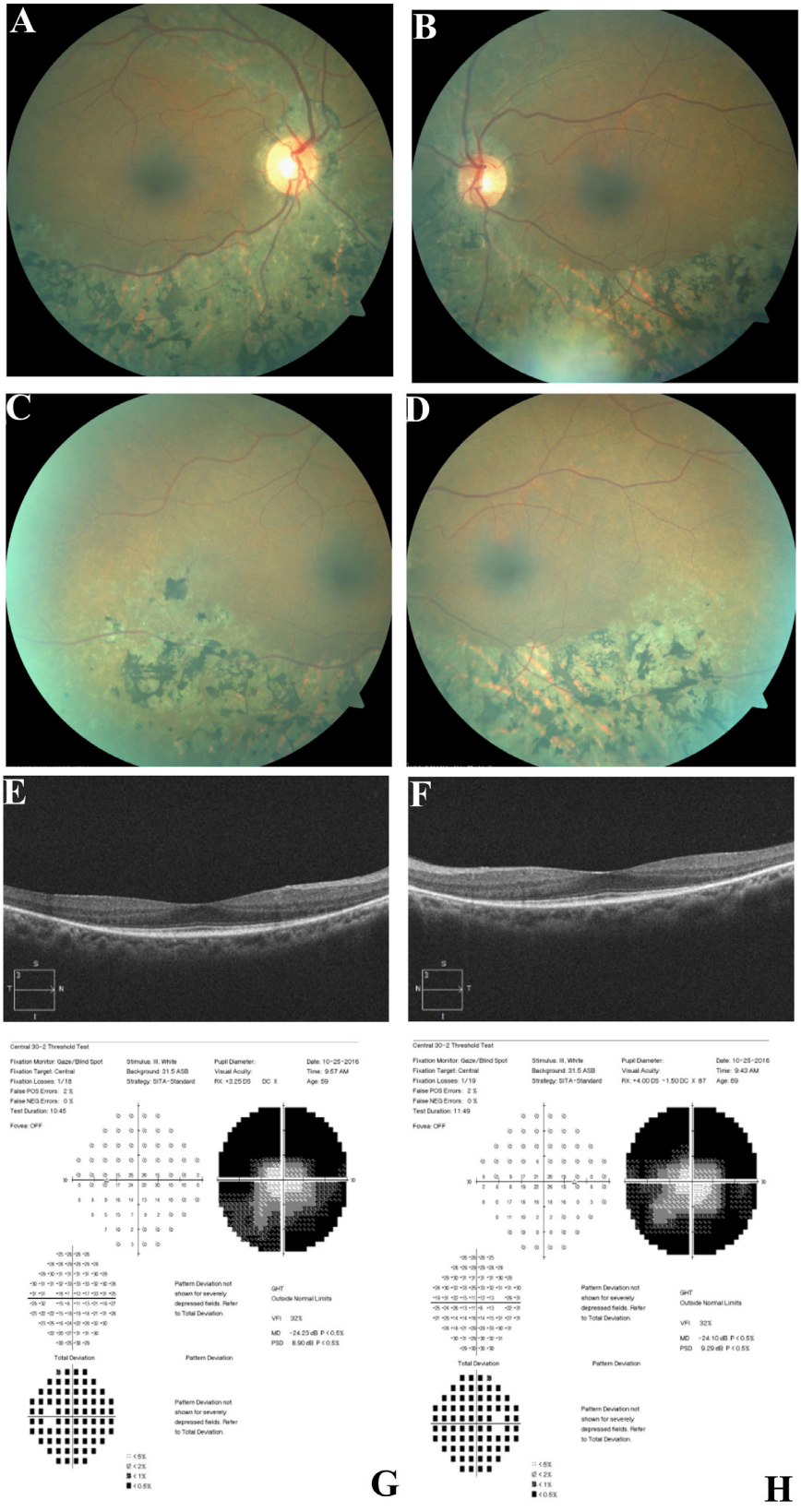

Figure 6. Clinical imagining of patient 6 with a c.44A>G mutation in *RHO* (p.Asn15Ser). **A**, **C**: Oculus dexter (OD) color photos of the posterior pole showing marked RPE atrophy and bone spicules adjacent to and along the inferior arcades with mild extension temporally to the fovea as well as superonasally with respect to the optic disc and the superior arcade. **B**, **D**: Oculus sinister (OS) color photos of the posterior pole showing marked RPE atrophy and bone spicules adjacent to and along the inferior arcades with mild extension temporally to the fovea as well as superonasally with respect to the optic disc and the superior arcade. **E**: OD foveal spectral-domain optical coherence tomography (SD-OCT) showing parafoveal retinal thinning and loss of the ellipsoid zone and photoreceptor layer most prominent in the inferior part of the posterior pole. **F**: OS foveal SD-OCT showing parafoveal retinal thinning and loss of the ellipsoid zone and photoreceptor layer most prominent in the inferior part of the posterior pole. **G**: OS Humphrey 30-2 SITA Standard visual field showing circumferential constriction. **H**: OD Humphrey 30-2 SITA Standard visual field showing circumferential constriction.

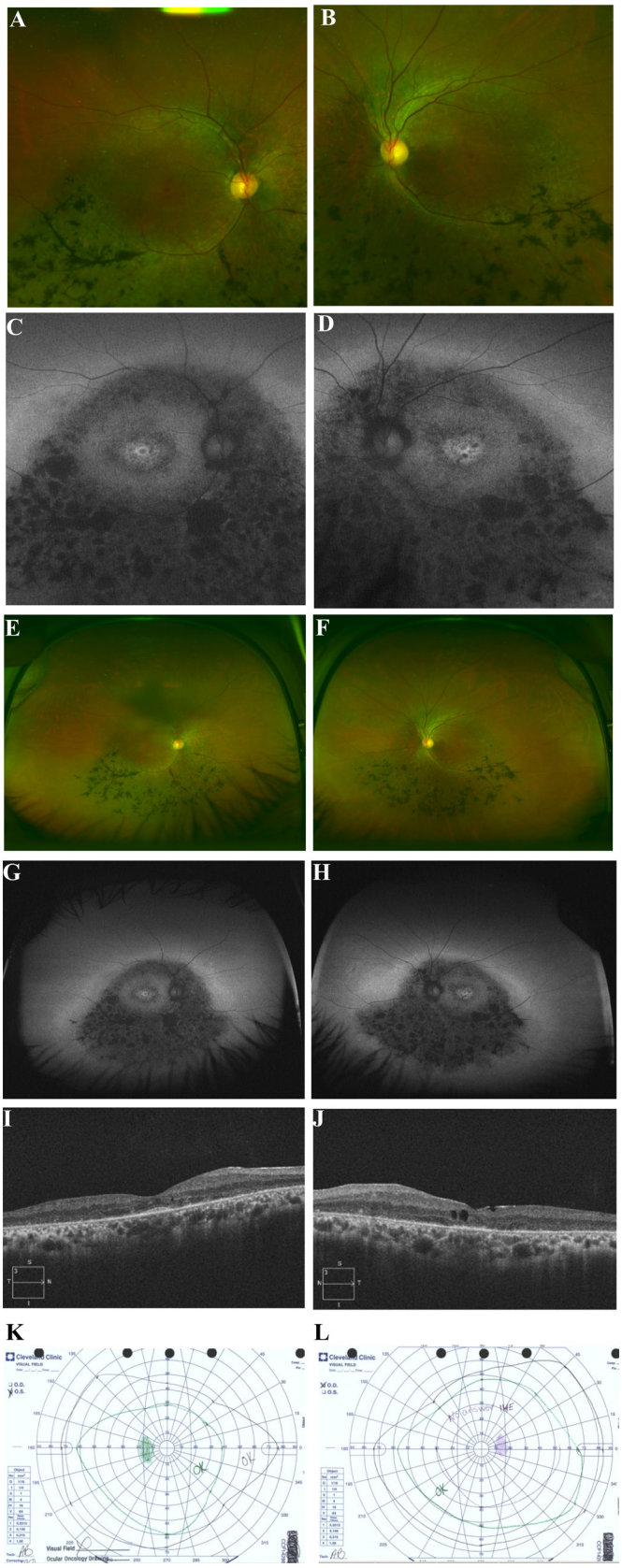

Figure 7. Clinical imagining of patient 7 with a c.44A>G mutation in *RHO* (p.Asn15Ser). **A**, **E**: Oculus dexter (OD) color photos showing a concentric foveal hypopigmentation, marked parafoveal RPE mottling and hypopigmentation, RPE atrophy, and bone spicules adjacent to and along the inferior arcades with mild extension temporally to the fovea as well as temporally and superonasally with respect to the optic disc and superonasally with respect to the superior arcade. **B**, **F**: Oculus sinister (OS) color photos showing concentric foveal hypopigmentation, marked parafoveal RPE mottling and hypopigmentation, RPE atrophy, and bone spicules adjacent to and along the inferior arcades with mild extension temporally to the fovea as well as temporally and superonasally with respect to the optic disc and superonasally with respect to the superior arcade. **C**, **G**: OD fundus autofluorescence (FAF) fundus photos showing a central hyperautofluorescence (hyperAF) rim surrounded by a speckled pattern of hypoautofluorescence (hypoAF) forming a "bull's eye"-like pattern. There is also a circinate area of hypoAF along the inferior and superior arcades with a patchy pattern of marked hypoAF extending inferiorly from the inferior arcade into the periphery. **D**, **H**: OS FAF fundus photos showing a central hyperAF rim surrounded by a speckled pattern of hypoAF forming a "bull's eye"-like pattern. There is also a circinate area of hypoAF along the inferior and superior arcades with a patchy pattern of marked hypoAF extending inferiorly from the inferior arcade into the periphery. **I**: OD foveal spectral-domain optical coherence tomography (SD-OCT) showing a small island of preservation in the ellipsoid zone subfoveally, marked retinal layers contour abnormalities and thinning, RPE hyperreflective round deposits, significant choroidal hyper-reflective signal, and intraretinal cystic spaces. **J**: OS foveal SD-OCT showing a small island of preservation in the ellipsoid zone subfoveally, marked retinal layer contour abnormalities and thinning, RPE hyperreflective round deposits, significant choroidal hyper-reflective signal, and intraretinal cystic spaces. **K**: OS Goldman visual field showing superonasal and inferonasal defects. **L**: OD Goldman visual field showing superonasal defects.

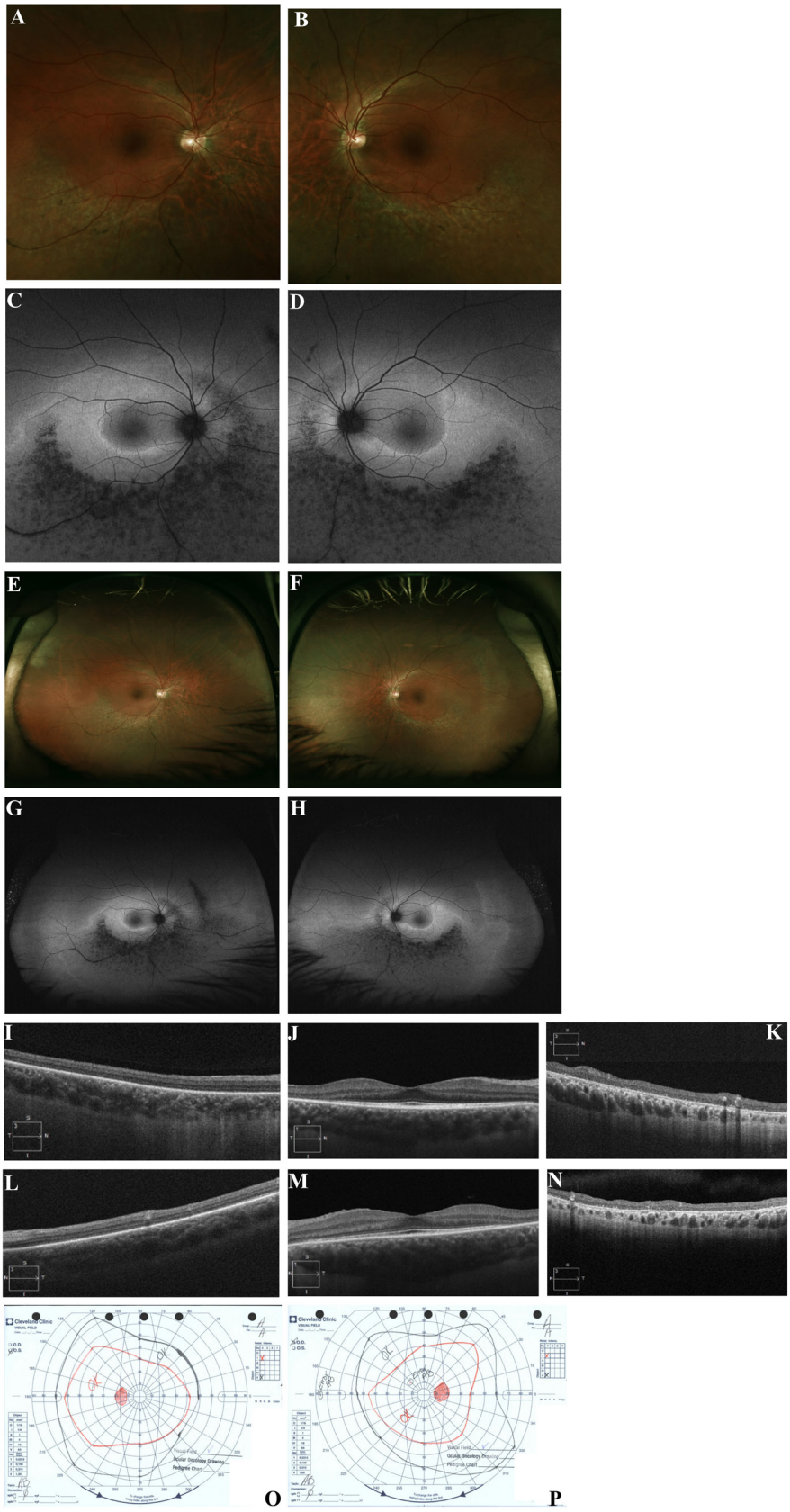

Figure 8. Clinical imagining of patient 8 with a c.325G>A mutation in *RHO* (p.Gly109Arg). **A**, **E**: Oculus dexter (OD) color photos showing RPE hypopigmentation and atrophic changes extending inferiorly from the inferior arcade border to the periphery. **B**, **F**: Oculus sinister (OS) color photos showing RP RPE hypopigmentation and atrophic changes extending inferiorly from the inferior arcade border to the periphery. **C**, **G**: OD fundus autofluorescence (FAF) fundus photos showing a linear hyper-autofluorescence (hyperAF) abutting the inferior edge of the fovea. An OU patchy pattern of hypoautofluorescence (hypoAF) extending from the inferior border of the inferior arcade into the inferior and inferonasal midperiphery. **D**, **H**: OS FAF fundus photos showing linear hyperAF abutting the inferior edge of the fovea. OU patchy pattern of hypoAF extending from the inferior border of the inferior arcade into the inferior and inferonasal midperiphery. **I**: OD spectral-domain optical coherence tomography (SD-OCT) of the superior posterior pole showing retinal thinning and ellipsoid zone loss of the superior posterior pole adjacent to the arcades. **J**: OD foveal SD-OCT showing a small island of preservation in the ellipsoid zone subfoveally with parafoveal loss of the ellipsoid zone. **K**: OD SD-OCT of the inferior posterior pole showing marked retinal disorganization and RPE hyper-reflective round deposits adjacent to the arcades with significant choroidal hyporeflective signal. **L**: OS SD-OCT of the superior posterior pole showing retinal thinning and ellipsoid zone loss adjacent to the arcades. **M**: OS foveal SD-OCT showing a small island of preservation in the ellipsoid zone subfoveally with parafoveal loss of the ellipsoid zone. **N**: OS SD-OCT of the inferior posterior pole showing marked retinal disorganization and RPE hyper-reflective round deposits adjacent to the arcades with significant choroidal hyporeflective signal. **O**: OS Goldman visual field showing mild nasal constriction. **P**: OD Goldman visual field showing small superior defects and mild temporal constriction.

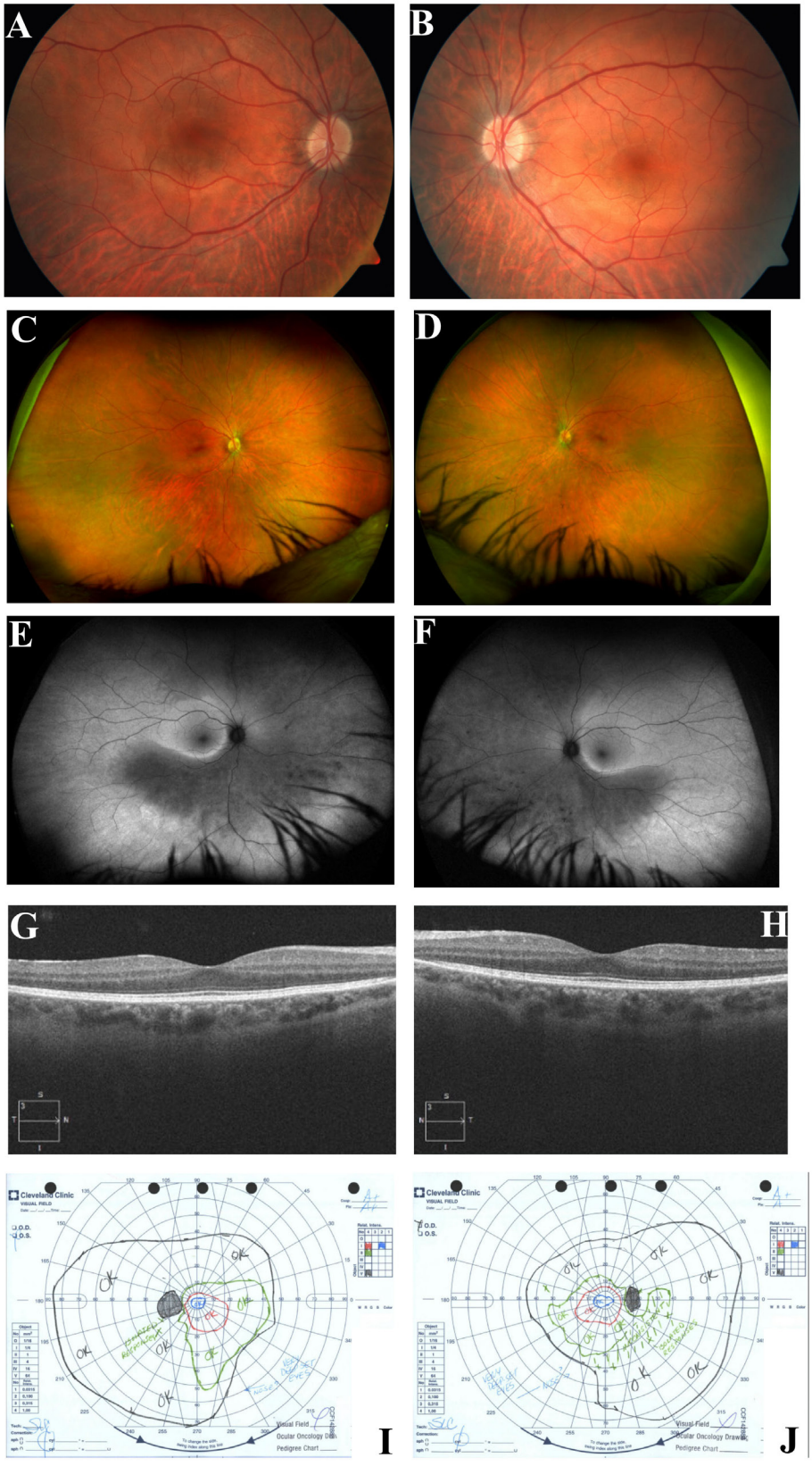

Figure 9. Clinical imagining of patient 9 with a c.68C>A mutation in *RHO* (p.Pro23His). **A**, **C**: Oculus dexter (OD) color photos showing scant bone spicules in the inferotemporal periphery. **B**, **D**: Oculus sinister (OS) color photos showing scant bone spicules in inferotemporal periphery. **E**: OD fundus autofluorescence (FAF) fundus photos showing a crescent-shaped area of hypoautofluorescence (hypoAF) along the inferior arcades extending into the inferior midperiphery as well as the infero- and superonasal periphery. **F**: OS FAF fundus photos showing a crescent-shaped area of hypoAF along the inferior arcades extending into the inferior midperiphery as well as the infero- and superonasal periphery. **G**: OD foveal spectral-domain optical coherence tomography (SD-OCT) showing mild outer retinal attenuation. **H**: OS foveal SD-OCT showing mild outer retinal attenuation. **I**: OS Goldman visual field showing circumferential constriction. **J**: OD Goldman visual field showing circumferential constriction.

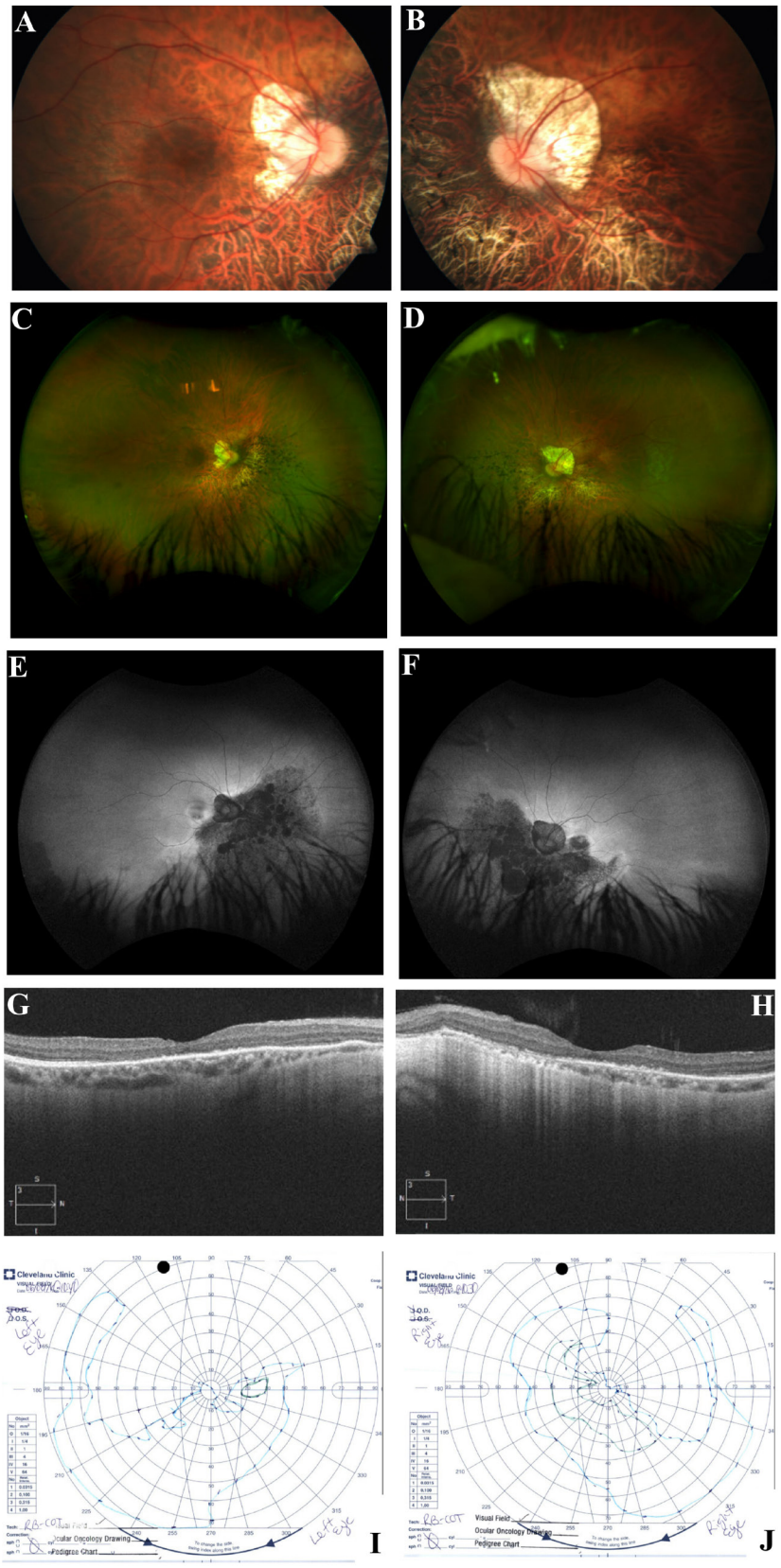

Figure 10. Clinical imagining of patient 10 with a c.3092_3093delAG mutation in *RPGR*. **A**, **C**: Oculus dexter (OD) color photos showing a tessellated fundus, blunted foveal reflex, hypopigmentation, and atrophic changes most prominent along the inferior arcades midperipherally. There are also marked bone spicules in the inferonasal midperiphery. **B**, **D**: Oculus sinister (OS) color photos showing a tessellated fundus, blunted foveal reflex, hypopigmentation, and atrophic changes most prominent along the inferior arcades midperipherally. There are also marked bone spicules in the inferonasal midperiphery. **E**: OD fundus autofluorescence (FAF) photo showing a hypoautofluorescence (hypoAF) area bordering the inferior arcades and extending inferiorly and inferonasally into the midperiphery. There is also a linear edge of hyper-autofluorescence (hyperAF) superior to the area of hypoAF. **F**: OS FAF photo showing a hypoAF area bordering the inferior arcades and extending inferiorly and inferonasally into the midperiphery. There is also a linear edge of hyperAF superior to the area of hypoAF. **G**: OD foveal spectral-domain optical coherence tomography (SD-OCT) showing generalized foveal thinning with marked ellipsoid zone abnormalities as well as RPE hyperreflective round deposits and diffuse thickening of the RPE band. **H**: OS foveal SD-OCT showing generalized foveal thinning with marked ellipsoid zone abnormalities, as well as RPE hyperreflective round deposits and diffuse thickening of the RPE band. **I**: OS Goldman visual field showing circumferential constriction with marked superior visual field defects. **J**: OD Goldman visual field showing circumferential constriction with marked superior visual field defects.

p.Thr58Arg and p.Thr58Met: Thr58 is located in helix 1 of rhodopsin. Functional analyses of p.Thr58Arg and p.Thr58Met mutants showed normal ultraviolet (UV)–visible absorption spectra specific to rhodopsin, suggesting a minor structural change in the rhodopsin molecule. However, significant structural changes have been reported in association with the mutants' ability to activate transducin [41]. Some residues, including Thr58 and Arg135, close to the transducin binding sites, Cys140, Lys141, Phe228, Thr229, and Val230 in the three-dimensional state of rhodopsin, could influence activation of transducin. In contrast, rhodopsin with R135W mutations, which can cause severe RP, displayed more impaired ability to activate transducin. p.Thr58Arg protein expressed in HEK293S cells showed decreased protein stability, decreased photobleaching spectra, mislocalization in the ER, and abnormal glycosylation [25].

p.Val87Asp: Val87 is located in helix 2 of rhodopsin. COS-1 cells expressing the p.Val87Asp rhodopsin mutant poorly regenerates with the visual chromophore, suggesting that Val87 involves interaction with 11-*cis*-retinal. Further, the p.Val87Asp mutant is thought to result in a less stable structural change [33].

p.Gly106Arg: Gly106 is located in the extracellular loop 1 between helix 2 and helix 3. p.Gly106Arg rhodopsin expressed in HEK293S cells showed an aberrant absorbance spectrum, mislocalization in the ER, and lower mobility of glycosylation, similar to other mutants, such as p.Thr17Met, p.Pro23His, and p.Asp190Arg [25].

p.Trp126Leu: Trp126 is located in helix 3. Cross-linking experiments with an analog of 11-*cis*-retinal revealed that Trp126 is one of major sites associated with chromophore

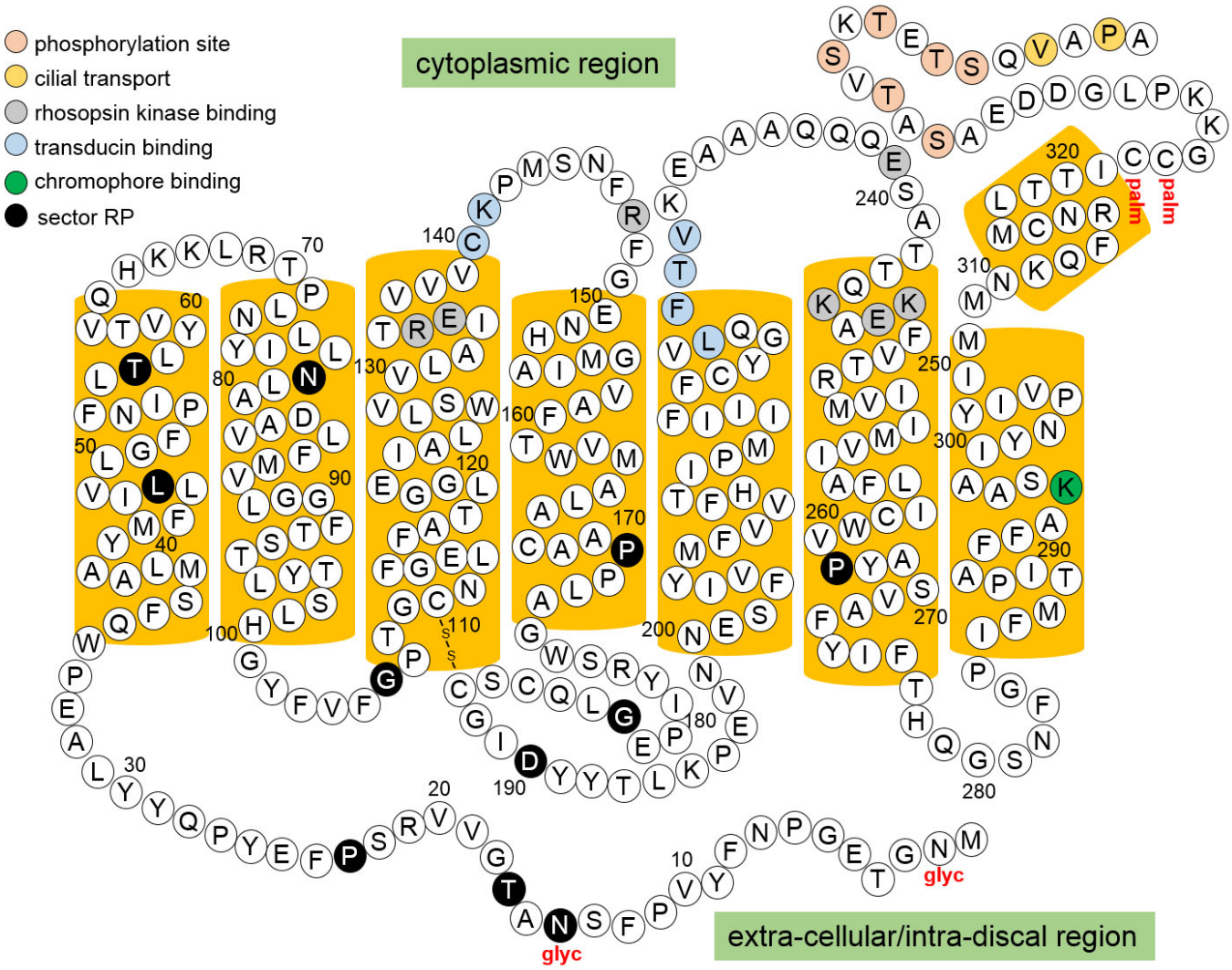

Figure 11. Illustration of mutations in *RHO* previously reported to cause sector RP.

binding and support a Schiff's base link between 11-*cis*-retinal and the Leu296 site [42]. In addition, protein modeling suggested that the p.Trp126Leu mutation likely affects the side-chain interaction between helix 3 and helix 6 in the light-adapted form [43]. These molecular modeling and simulation findings suggest that the p.Trp126Leu mutation may impair rhodopsin function by affecting its conformational transition in the light-adapted form. The p.Trp126Leu of bovine rhodopsin also showed weaker G-protein activation [44].

p.Gly182Ser: Gly182 is located in extracellular loop 2 between helix 4 and helix 5. Although the p.Gly182Ser mutation has not been examined biochemically, the adjacent amino acid mutation p.Glu181Lys was studied. Photoreceptor cells differentiated from induced pluripotent stem cells (iPSCs) established from a patient with RP with the p.Glu181Lys mutation showed degeneration by the fifth week of the culture due to apoptosis and impaired autophagy [45]. Because treatment with salubrinal, a selective inhibitor of eIF2α, leads to an increased number of iPSC-derived rod photoreceptor cells, and because the treated cells showed reduced levels of ER stress and apoptotic markers, the authors of this last paper suggested that rod photoreceptor cell death caused by the p.Glu181Lys mutation could be suppressed by inhibiting protein synthesis, including that of abnormal rhodopsin. Specifically, Yoshida et al. proved that treatment with NQDI-1, an inhibitor of ASK1 activation, increased the survival of mutant rod photoreceptor cells, which is consistent with the hypothesis that apoptosis is regulated by the ER stress-induced Ire-1α-ASK1-JNK pathway [46].

p.Asp190Asn and p.Asp190Gly: Asp190 is a highly conserved ion pair at the ends of loop E-2, and Asp190 and Arg177 are the conserved ion pair. The Arg-177/Asp-190 ion pair is critical for the folding and stability of dark-state rhodopsin [47]. The p.Asp190Asn mutation dramatically altered the stability of the retinal Schiff's base in dark-state rhodopsin but did not affect the Meta II state [48]. Some individuals with heterozygous p.Asp190Asn mutations were asymptomatic, especially in childhood [49]. A KI mouse model of p.Asp190Asn was previously developed [50]. The heterogynous p.Asp190Asn mouse did not show obvious retinal changes at 21 days of age, but photoreceptor degeneration was documented with ERG and histological evaluation at 210 days. However, the retinal degeneration was not considered severe. ER stresses by p.Asp190Asn mutant rhodopsin have been suggested [33], but accumulation of the mutant rhodopsin was not detected in the KI mice. The p.Asp190Gly protein, which causes adRP, expressed in the HEK293S cells showed decreased protein stability, decreased photobleaching spectrum, mislocalization in the ER, and abnormal glycosylation [25].

DISCUSSION

Sector RP has been reported in patients with mutations in *RHO*, *USH1C,* and *CDH23* [51]. This report presented novel mutations in the *RHO* and *RPGR* genes associated with this uncommon retinal phenotype and reviewed the literature on the subject with an emphasis on the biochemical effects of the individual rhodopsin mutations on the protein and any animal models in which these mutations have been tested.

From a phenotypic perspective, sector RP is characterized by more severe retinal degeneration with RPE pigmentary changes, or atrophy, or both along the inferior arcades and in the inferior part of the fundus. This pattern of degeneration is most noticeable on the FAF examination and corresponds to superior visual defects on visual field testing. All patients in the present study displayed this pattern. Due to the central foveal sparing of the disease, all patients with mutations in *RHO* maintained excellent visual acuity in both eyes. Patient 10 with the c.3092_3093delAG mutation in *RPGR,* however, showed severe generalized foveal thinning and contour atrophy that corresponds to and explains his poor VA. The severity of this phenotypic variation difference could be explained by the severity of the deleterious aspect of the causal *RPGR* mutation compared to a resultant missense in the reported *RHO* mutations. Although in most cases the pattern was bilateral and symmetric, some patients demonstrated some degree of asymmetry as noted on multimodal imaging.

Sector RP is most commonly associated with mutations in rhodopsin, a G-protein coupled receptor that consists of a 348-amino acid rod opsin and a visual chromophore, 11-*cis*-retinal [52]. Rhodopsin is found in rod photoreceptor cells and is localized to the discs of the outer segment [53]. The visual chromophore 11-*cis*-retinal is photoisomerized to all-*trans*-retinal by photon absorption, and this conformational change initiates rhodopsin activation, which further activates a cascade of biochemical reactions referred to as the phototransduction cascade [54] Currently, there are numerous mutations in rhodopsin reported to result in classic or sector RP (RetNet).

Cideciyan et al. proposed two main phenotypic classes (A and B) of adRP caused by rhodopsin mutations. Class A mutations lead to severe diffuse abnormal rod function early in life, while in class B mutations, the rods have nearly normal function, even in adult patients, and there is a slow disease progression with a specific inferior-to-superior gradient of disease vulnerability to retinal degenerative processes [55]. This gradient tends to be diagonal across the retina, most severe in the pericentral and inferonasal retina. Cideciyan et al. included the following protein changes p.Thr17Met,

p.Pro23His, p.Thr58Arg, p.Val87Asp, p.Gly106Arg, and p.Asp190Gly in the Class B category. Interestingly, all amino acid rhodopsin mutations in Class B disease except Val87 have been reported to cause sector RP. Additionally, retinal degeneration in sector RP is observed in areas adjacent to the vascular arcade of the inferior retina. Predominant retinal degeneration was observed in the inferior retina of the p.Pro23His KI mouse [18]. Interestingly, knockout mice with heterozygous p. Pro23His rhodopsin mutations also show milder retinal degeneration phenotypes compared to homozygous mice [56], mirroring the human disease with a milder phenotype like that seen in sector RP.

The exact pathogenesis of sector RP remains presently unknown. While the diagnosis of sector RP is clinical and based on a "pattern," there is evidence that the preferential inferior involvement is the result of certain rhodopsin mutations, and that it is a defined entity that reflects an underlying pathophysiological disturbance. Some evidence suggests that light exposure could lead to retinal degeneration and thus, contribute to the pathogenesis of RP. Noell and Albrecht showed that the absorbance spectrum of rod photoreceptor visual pigment, rhodopsin, coincided with the phototoxic wavelengths of light [57]. *Rpe65* knockout mice, in which there is misfolded, mislocalized, or aggregated rhodopsin, were reported to resist the light-induced apoptosis of phototoxic damage [58]. This phenomenon is possibly related to the inability of mutant rhodopsin to exit the endoplasmic reticulum resulting in prolonged intracellular stress, and thus, apoptosis-mediated signaling during light exposure [59-62].

It has been postulated that the faster retinal degeneration progression in the inferior retina of patients with sector RP could be due to free radical-mediated apoptosis secondary to light exposure preferentially affecting the inferior retina [63-65]. In general, the inferior retina receives more light exposure due to the more elevated location of most light sources (sunlight and ceiling lighting). After calculating the dose distribution of blue light on the retinal surface, Schwartz et al. reported a noticeable greater effect on the superior visual field compared to the inferior one [65]. The authors reported that the highest dose of UV and blue light is located 4 mm superior to the macula on the visual field [65].

The phenotypic difference between the superior and inferior retina with respect to light exposure could be related to an abnormal blue light variation in retinal sensitivity [65]. Interestingly, using Tübinger perimeter-based psychophysical testing, Fishman et al. demonstrated marked threshold differences between the superior and inferior retina in patients with p.Thr17Met and p.Gly182Ser mutations in *RHO* causing sector RP [66]. Furthermore, Grover et al. reported an early preferential superior visual field predilection in a certain patient with RP [67]. Based on this information, it is then possible for patients with rhodopsin-disease causing mutations to have more advanced retinal degeneration and photoreceptor loss occur in the inferior retina [62,63]. By the same logic, exposure to a darkened environment has been shown to slow the rate of retinal degeneration in P23H rats and eliminate the degenerative changes between the inferior and superior retina [6,7].

In this study, we report a novel p.Leu226Pro (patients 2 and 3) mutation in rhodopsin causing sector RP. The p.Leu226Pro mutation involves one of binding sites of retinal G-protein, transducin, and p.Ser270 potentially affects visual chromophore binding as described in the section above. Both residues play a key role in rhodopsin functions. Interestingly transducin can bind six residues in rhodopsin (Figure 7), and until now, mutations in these residues have not been reported to cause RP. Although p.Leu226 is a transducin-binding site, and physiologically plays an important role in rhodopsin function, the p.Leu226Pro mutation reported in this study resulted in only a mild type of RP, that is, sector RP. This could possibly be explained by the redundancy of the six residues. Similarly, because p.Ser270Arg mildly affects chromophore binding, this mutation might cause only sector RP. These two mutations should be also categorized as Class B [55].

Some *RHO*-induced adRP animal models showed more severe retinal degeneration in the inferior retina [6,7]. This regional difference in degenerative vulnerability seemed to somehow depend on the animal model being investigated. For instance, degeneration induced by the photoreceptor toxin iodoacetic acid was more severe in the inferior retina of rabbits [68]. Furthermore, *Crb1* mice also showed retinal degeneration only in the inferior retina [69]. In the *rd/rd* mouse model, however, there were significantly more cones that survived in the inferior than in the superior hemisphere in most retinas [70]. Additionally, light-induced retinal damage in albino rats was reported to be more severe in the superior retina [71,72].

In an attempt to investigate regional differences in photoreceptor degeneration, Zhu et al. quantified gene expression or regulation in the C57BL/6J mouse retina after exposure to hyperoxia [73]. Genes related to light-induced apoptosis and cytoprotection, as well as immune protective and inflammatory processes, were found to be significantly more regulated in the inferior retina [73]. It is then possible that the inferior retinal vulnerability to light could share similar biomolecular pathways as those seen in the hyperoxic environment, and thus, explain the robustness of the superior retina.

Rod photoreceptors are more sensitive to light-induced damage than cones [74]. Rod density is highest at 20 to 30 degrees from the center of the human retina, which corresponds to the perivascular arcade area. Production of oxygen-associated free radicals plays an important role in retinal phototoxicity [75]. Furthermore, photoactivated visual chromophore all-*trans*-retinal, which is produced in the photoreceptors after photoisomerization of 11-*cis*-retinal, is detrimental when its metabolism is impaired [76]. Studies of rhodopsin-induced sector RP implicated a critical role of light exposure in the pathogenesis of the degenerative process [59-62]. It has been suggested that the inferonasal quadrant is most commonly affected in sector RP due to the greater light exposure of the lower retina from an overhead light source [3]. Taking these observations into consideration, the inferior retina along the vascular arcade appears to be most vulnerable to light-induced stresses, and thus, the inferior sectoral degeneration in individuals carrying heterozygous Class B rhodopsin mutations.

Based on a review of the literature and the cases in this report, we believe that sector RP is a well-defined clinical entity with relative preservation of the superior areas of the retina and fields of vision as evident by the multimodal imaging and visual field testing. Despite this milder phenotype, the disease does progress over time. There are currently no formal natural history studies available to investigate the rate of progression over time, or studies of any treatment approaches for patients with this clinical type of RP.

APPENDIX 1. CLINICAL CHARACTERISTICS AND MOLECULAR PATHOLOGIC FEATURES OF PATIENTS IN PRESENT STUDY.

To access the data, click or select the words "Appendix 1." Abbreviations: OD: oculus dexter, OS: oculus sinister, OU: oculus uterque, FAF: fundus autofluorescence, AF: autofluorescence, ERG : electroretinogram.

ACKNOWLEDGMENT

We have no relevant funding resources to disclose in relation to this study. We would like to thank all of our patients for their willingness to participate in our study

REFERENCES

1. Daiger SP, Sullivan LS, Bowne SJ. Genes and mutations causing retinitis pigmentosa. Clin Genet 2013; 84:132-41. [PMID: 23701314].

2. O'Neal TB, Luther EE. Retinitis Pigmentosa. StatPearls. Treasure Island (FL): StatPearls Publishing; 2018.

3. Napier ML, Durga D, Wolsley CJ, Chamney S, Alexander S, Brennan R, Simpson DA, Silvestri G, Willoughby CE. Mutational Analysis of the Rhodopsin Gene in Sector Retinitis Pigmentosa. Ophthalmic Genet 2015; 36:239-43. [PMID: 25265376].

4. Sullivan LS, Bowne SJ, Birch DG, Hughbanks-Wheaton D, Heckenlively JR, Lewis RA, Garcia CA, Ruiz RS, Blanton SH, Northrup H, Gire AI, Seaman R, Duzkale H, Spellicy CJ, Zhu J, Shankar SP, Daiger SP. Prevalence of disease-causing mutations in families in families with autosomal dominant retinitis pigmentosa: a screen of known genes in 200 families. Invest Ophthalmol Vis Sci 2006; 47:3052-64. [PMID: 16799052].

5. Tam BM, Moritz OL. Dark rearing rescues P23H rhodopsin-induced retinal degeneration in a transgenic Xenopus laevis model of retinitis pigmentosa: a chromophore-dependent mechanism characterized by production of N-terminally truncated mutant rhodopsin. J Neurosci 2007; 27:9043-53. [PMID: 17715341].

6. Naash ML, Peachey NS, Li ZY, Gryczan CC, Goto Y, Blanks J, Milam AH, Ripps H. Light-induced acceleration of photoreceptor degeneration in transgenic mice expressing mutant rhodopsin. Invest Ophthalmol Vis Sci 1996; 37:775-82. [PMID: 8603862].

7. Organisciak DT, Darrow RM, Barsalou L, Kutty RK, Wiggert B. Susceptibility to retinal light damage in transgenic rats with rhodopsin mutations. Invest Ophthalmol Vis Sci 2003; 44:486-92. [PMID: 12556372].

8. Galy A, Roux MJ, Sahel JA, Leveillard T, Giangrande A. Rhodopsin maturation defects induce photoreceptor death by apoptosis: a fly model for RhodopsinPro23His human retinitis pigmentosa. Hum Mol Genet 2005; 14:2547-57. [PMID: 16049034].

9. Li T, Sandberg MA, Pawlyk BS, Rosner B, Hayes KC, Dryja TP, Berson EL. Effect of vitamin A supplementation on rhodopsin mutants threonine-17–> methionine and proline-347–> serine in transgenic mice and in cell cultures. Proc Natl Acad Sci USA 1998; 95:11933-8. .

10. Tam BM, Noorwez SM, Kaushal S, Kono M, Moritz OL. Photoactivation-induced instability of rhodopsin mutants T4K and T17M in rod outer segments underlies retinal degeneration in X. laevis transgenic models of retinitis pigmentosa. J Neurosci 2014; 34:13336-48. .

11. Sancho-Pelluz J, Tosi J, Hsu CW, Lee F, Wolpert K, Tabacaru MR, Greenberg JP, Tsang SH, Lin CS. Mice with a D190N mutation in the gene encoding rhodopsin: a model for human autosomal-dominant retinitis pigmentosa. Mol Med 2012; 9:549-55. [PMID: 22252712].

12. Sohocki MM, Daiger SP, Bowne SJ, Rodriquez JA, Northrup H, Heckenlively JR, Birch DG, Mintz-Hittner H, Ruiz RS, Lewis RA, Saperstein DA, Sullivan LS. Prevalence of mutations causing retinitis pigmentosa and other inherited retinopathies. Hum Mutat 2001; 17:42-51. [PMID: 11139241].

13. Dryja TP, McGee TL, Reichel E, Hahn LB, Cowley GS, Yandell DW, Sandberg MA, Berson EL. A point mutation

of the rhodopsin gene in one form of retinitis pigmentosa. Nature 1990; 343:364-6. [PMID: 2137202].

14. Olsson JE, Gordon JW, Pawlyk BS, Roof D, Hayes A, Molday RS, Mukai S, Cowley GS, Berson EL, Dryja TP. Transgenic mice with a rhodopsin mutation (Pro23His): a mouse model of autosomal dominant retinitis pigmentosa. Neuron 1992; 9:815-30. [PMID: 1418997].

15. Naash MI, Ripps H, Li S, Goto Y, Peachey NS. Polygenic disease and retinitis pigmentosa: albinism exacerbates photoreceptor degeneration induced by the expression of a mutant opsin in transgenic mice. J Neurosci 1996; 16:7853-8. [PMID: 8987813].

16. Lewin AS, Drenser KA, Hauswirth WW, Nishikawa S, Yasumura D, Flannery JG, LaVail MM. Ribozyme rescue of photoreceptor cells in a transgenic rat model of autosomal dominant retinitis pigmentosa. Nat Med 1998; 4:967-71. [PMID: 9701253].

17. Scott PA, Fernandez de Castro JP, Kaplan HJ, McCall MAA. Pro23His mutation alters prenatal rod photoreceptor morphology in a transgenic swine model of retinitis pigmentosa. Invest Ophthalmol Vis Sci 2014; 55:2452-9. [PMID: 24618321].

18. Sakami S, Maeda T, Bereta G, Okano K, Golczak M, Sumaroka A, Roman AJ, Cideciyan AV, Jacobson SG, Palczewski K. Probing mechanisms of photoreceptor degeneration in a new mouse model of the common form of autosomal dominant retinitis pigmentosa due to P23H opsin mutations. J Biol Chem 2011; 286:10551-67. [PMID: 21224384].

19. Sakami S, Kolesnikov AV, Kefalov VJ, Palczewski K. P23H opsin knock-in mice reveal a novel step in retinal rod disc morphogenesis. Hum Mol Genet 2014; 23:1723-41. [PMID: 24214395].

20. Batten ML, Imanishi Y, Maeda T, Tu DC, Moise AR, Bronson D, Possin D, Van Gelder RN, Baehr W, Palczewski K. Lecithin-retinol acyltransferase is essential for accumulation of all-trans-retinyl esters in the eye and in the liver. J Biol Chem 2004; 279:10422-32. [PMID: 14684738].

21. Frederick JM, Krasnoperova NV, Hoffmann K, Church-Kopish J, Rüther K, Howes K, Lem J, Baehr W. Mutant rhodopsin transgene expression on a null background. Invest Ophthalmol Vis Sci 2001; 42:826-33. [PMID: 11222546].

22. Tam BM, Moritz OL. Characterization of rhodopsin P23H-induced retinal degeneration in a Xenopus laevis model of retinitis pigmentosa. Invest Ophthalmol Vis Sci 2006; 47:3234-41. [PMID: 16877386].

23. Tam BM, Qazalbash A, Lee HC, Moritz OL. The dependence of retinal degeneration caused by the rhodopsin P23H mutation on light exposure and vitamin a deprivation. Invest Ophthalmol Vis Sci 2010; 51:1327-34. [PMID: 19933196].

24. Chen Y, Jastrzebska B, Cao P, Zhang J, Wang B, Sun W, Yuan Y, Feng Z, Palczewski K. Inherent instability of the retinitis pigmentosa P23H mutant opsin. J Biol Chem 2014; 289:9288-303. [PMID: 24515108].

25. Sung CH, Schneider BG, Agarwal N, Papermaster DS, Nathans J. Functional heterogeneity of mutant rhodopsins responsible for autosomal dominant retinitis pigmentosa. Proc Natl Acad Sci USA 1991; 88:8840-4. [PMID: 1924344].

26. Janz JM, Farrens DL. Role of the retinal hydrogen bond network in rhodopsin Schiff base stability and hydrolysis. J Biol Chem 2004; 279:55886-94. [PMID: 15475355].

27. Sheikh SP, Zvyaga TA, Lichtarge O, Sakmar TP, Bourne HR. Rhodopsin activation blocked by metal-ion-binding sites linking transmembrane helices C and F. Nature 1996; 383:347-50. [PMID: 8848049].

28. Ye S, Zaitseva E, Caltabiano G, Schertler GF, Sakmar TP, Deupi X, Vogel R. Tracking G-protein-coupled receptor activation using genetically encoded infrared probes. Nature 2010; 464:1386-9. [PMID: 20383122].

29. Eilers M, Goncalves JA, Ahuja S, Kirkup C, Hirshfeld A, Simmerling C, Reeves PJ, Sheves M, Smith SO. Structural transitions of transmembrane helix 6 in the formation of metarhodopsin I. J Phys Chem B 2012; 116:10477-89. [PMID: 22564141].

30. Sung CH, Davenport CM, Nathans J. Rhodopsin mutations responsible for autosomal dominant retinitis pigmentosa. Clustering of functional classes along the polypeptide chain. J Biol Chem 1993; 268:26645-9. [PMID: 8253795].

31. Hwa J, Garriga P, Liu X, Khorana HG. Structure and function in rhodopsin: packing of the helices in the transmembrane domain and folding to a tertiary structure in the intradiscal domain are coupled. Proc Natl Acad Sci USA 1997; 94:10571-6. [PMID: 9380676].

32. Kaushal S, Ridge KD, Khorana HG. Structure and function in rhodopsin: the role of asparagine-linked glycosylation. Proc Natl Acad Sci USA 1994; 91:4024-8. [PMID: 8171029].

33. Kaushal S, Khorana HG. Structure and function in rhodopsin. 7. Point mutations associated with autosomal dominant retinitis pigmentosa. Biochemistry 1994; 33:6121-8. [PMID: 8193125].

34. Tam BM, Moritz OL. The role of rhodopsin glycosylation in protein folding, trafficking, and light-sensitive retinal degeneration. J Neurosci 2009; 29:15145-54. [PMID: 19955366].

35. Kijas JW, Miller BJ, Pearce-Kelling SE, Aguirre GD, Acland GM. Canine models of ocular disease: outcross breedings define a dominant disorder present in the English mastiff and bull mastiff dog breeds. J Hered 2003; 94:27-30. [PMID: 12692159].

36. Zhu L, Jang GF, Jastrzebska B, Filipek S, Pearce-Kelling SE, Aguirre GD, Stenkamp RE, Acland GM, Palczewski K. A naturally occurring mutation of the opsin gene (T4R) in dogs affects glycosylation and stability of the G protein-coupled receptor. J Biol Chem 2004; 279:53828-39. [PMID: 15459196].

37. Hildebrand PW, Scheerer P, Park JH, Choe HW, Piechnick R, Ernst OP, Hofmann KP, Heck M. A ligand channel through the G protein coupled receptor opsin. PLoS One 2009; 4:e4382-[PMID: 19194506].

38. Ramon E, Cordomi A, Aguila M, Srinivasan S, Dong X, Moore AT, Webster AR, Cheetham ME, Garriga P. Differential light-induced responses in sectorial inherited retinal degeneration. J Biol Chem 2014; 289:35918-28. [PMID: 25359768].

39. Ciarkowski J, Drabik P, Gieldon A, Kazmierkiewicz R, Slusarz R. Signal transmission via G protein-coupled receptors in the light of rhodopsin structure determination. Acta Biochim Pol 2001; 48:1203-7. [PMID: 11995993].

40. Sealfon SC, Chi L, Ebersole BJ, Rodic V, Zhang D, Ballesteros JA, Weinstein H. Related contribution of specific helix 2 and 7 residues to conformational activation of the serotonin 5–HT2A receptor. J Biol Chem 1995; 270:16683-8. [PMID: 7622478].

41. Min KC, Zvyaga TA, Cypess AM, Sakmar TP. Characterization of mutant rhodopsins responsible for autosomal dominant retinitis pigmentosa. Mutations on the cytoplasmic surface affect transducin activation. J Biol Chem 1993; 268:9400-4. [PMID: 8486634].

42. Nakayama TA, Khorana HG. Orientation of retinal in bovine rhodopsin determined by cross-linking using a photoactivatable analog of 11-cis-retinal. J Biol Chem 1990; 265:15762-9. [PMID: 2144289].

43. Katagiri S, Hayashi T, Akahori M, Itabashi T, Nishino J, Yoshitake K, Furuno M, Ikeo K, Okada T, Tsuneoka H, Iwata T. RHO Mutations (p.W126L and p.A346P) in Two Japanese Families with Autosomal Dominant Retinitis Pigmentosa. J Ophthalmol 2014; 2014:210947-[PMID: 25485142].

44. Nakayama TA, Khorana HG. Mapping of the amino acids in membrane-embedded helices that interact with the retinal chromophore in bovine rhodopsin. J Biol Chem 1991; 266:4269-75. [PMID: 1999419].

45. Yoshida T, Ozawa Y, Suzuki K, Yuki K, Ohyama M, Akamatsu W, Matsuzaki Y, Shimmura S, Mitani K, Tsubota K, Okano H. The use of induced pluripotent stem cells to reveal pathogenic gene mutations and explore treatments for retinitis pigmentosa. Mol Brain 2014; 7:45-[PMID: 24935155].

46. Yoshida T, Ozawa Y, Suzuki K, Yuki K, Ohyama M, Akamatsu W, Matsuzaki Y, Shimmura S, Mitani K, Tsubota K, Okano H. The use of induced pluripotent stem cells to reveal pathogenic gene mutations and explore treatments for retinitis pigmentosa. Mol Brain 2014; 7:45-.

47. Janz JM, Fay JF, Farrens DL. Stability of dark state rhodopsin is mediated by a conserved ion pair in intradiscal loop E-2. J Biol Chem 2003; 278:16982-91. [PMID: 12547830].

48. Janz JM, Farrens DL. Assessing structural elements that influence Schiff base stability: mutants E113Q and D190N destabilize rhodopsin through different mechanisms. Vision Res 2003; 43:2991-3002. [PMID: 14611935].

49. Tsui I, Chou CL, Palmer N, Lin CS, Tsang SH. Phenotype-genotype correlations in autosomal dominant retinitis pigmentosa caused by RHO, D190N. Curr Eye Res 2008; 33:1014-22. [PMID: 19085385].

50. Sancho-Pelluz J, Tosi J, Hsu CW, Lee F, Wolpert K, Tabacaru MR, Greenberg JP, Tsang SH, Lin CS. Mice with a D190N mutation in the gene encoding rhodopsin: a model for human autosomal-dominant retinitis pigmentosa. Mol Med 2012; 18:549-55. [PMID: 22252712].

51. Branson SV, McClintic JI, Stamper TH, Haldeman-Englert CR, John VJ. Sector Retinitis Pigmentosa Associated With Novel Compound Heterozygous Mutations of CDH23. Ophthalmic Surg Lasers Imaging Retina 2016; 47:183-6. [PMID: 26878454].

52. Nathans J, Hogness DS. Isolation and nucleotide sequence of the gene encoding human rhodopsin. Proc Natl Acad Sci USA 1984; 81:4851-5. [PMID: 6589631].

53. Goldberg AF, Moritz OL, Williams DS. Molecular basis for photoreceptor outer segment architecture. Prog Retin Eye Res 2016; 55:52-81. [PMID: 27260426].

54. Palczewski K. Chemistry and biology of vision. J Biol Chem 2012; 287:1612-9. [PMID: 22074921].

55. Cideciyan AV, Hood DC, Huang Y, Banin E, Li ZY, Stone EM, Milam AH, Jacobson SG. Disease sequence from mutant rhodopsin allele to rod and cone photoreceptor degeneration in man. Proc Natl Acad Sci USA 1998; 95:7103-8. [PMID: 9618546].

56. Liang Y, Fotiadis D, Maeda T, Maeda A, Modzelewska A, Filipek S, Saperstein DA, Engel A, Palczewski K. Rhodopsin signaling and organization in heterozygote rhodopsin knockout mice. J Biol Chem 2004; 279:48189-96. [PMID: 15337746].

57. Noell WK, Albrecht R. Irreversible Effects of Visible Light on the Retina: Role of Vitamin A. Science 1971; 172:76-80. [PMID: 5546288].

58. Grimm C, Wenzel A, Hafezi F, Yu S, Redmond TM, Remé CE. Protection of Rpe65-deficient mice identifies rhodopsin as a mediator of light-induced retinal degeneration. Nat Genet 2000; 25:63-6. [PMID: 10802658].

59. Schroder M, Kaufman RJ. The mammalian unfolded protein response. Annu Rev Biochem 2005; 74:739-89. [PMID: 15952902].

60. Alfinito PD, Townes-Anderson E. Activation of mislocalized opsin kills rod cells: a novel mechanism for rod cell death in retinal disease. Proc Natl Acad Sci USA 2002; 99:5655-60. [PMID: 11943854].

61. Lin JH, Li H, Yasumura D, Cohen HR, Zhang C, Panning B, Shokat KM, Lavail MM, Walter P. IRE1 signaling affects cell fate during the unfolded protein response. Science 2007; 318:944-9. [PMID: 17991856].

62. Paskowitz DM, LaVail MM, Duncan JL. Light and inherited retinal degeneration. Br J Ophthalmol 2006; 90:1060-6. [PMID: 16707518].

63. Jacobson SG, Acland GM, Aguirre GD, Aleman TS, Schwartz SB, Cideciyan AV, Zeiss CJ, Komaromy AM, Kaushal S, Roman AJ, Windsor EA, Sumaroka A, Pearce-Kelling SE, Conlon TJ, Chiodo VA, Boye SL, Flotte TR, Maguire AM, Bennett J, Hauswirth WW. Safety of recombinant

adeno-associated virus type 2–RPE65 vector delivered by ocular subretinal injection. Mol Ther 2006; 13:1074-84. [PMID: 16644289].

64. McDonald HR, Schatz H, Johnson RN. Ocular phototoxicity. Curr Opin Ophthalmol 1990; 1:280-4. .

65. Schwartz L, Boëlle PY, D'hermies F, Ledanois G, Virmont J. Blue light dose distribution and retinitis pigmentosa visual field defects: an hypothesis. Med Hypotheses 2003; 60:644-9. [PMID: 12710896].

66. Fishman GA, Stone EM, Sheffield VC, Gilbert LD, Kimura AE. Ocular findings associated with rhodopsin gene codon 17 and codon 182 transition mutations in dominant retinitis pigmentosa. Arch Ophthalmol 1992; 110:54-62. [PMID: 1731723].

67. Grover S, Fishman GA, Brown J Jr. Patterns of visual field progression in patients with retinitis pigmentosa. Ophthalmology 1998; 105:1069-75. [PMID: 9627658].

68. Liang L, Katagiri Y, Franco LM, Yamauchi Y, Enzmann V, Kaplan HJ, Sandell JH. Long-term cellular and regional specificity of the photoreceptor toxin, iodoacetic acid (IAA), in the rabbit retina. Vis Neurosci 2008; 25:167-77. [PMID: 18442439].

69. Mehalow AK, Kameya S, Smith RS, Hawes NL, Denegre JM, Young JA, Bechtold L, Haider NB, Tepass U, Heckenlively JR, Chang B, Naggert JK, Nishina PM. CRB1 is essential for external limiting membrane integrity and photoreceptor morphogenesis in the mammalian retina. Hum Mol Genet 2003; 12:2179-89. [PMID: 12915475].

70. LaVail MM, Matthes MT, Yasumura D, Steinberg RH. Variability in rate of cone degeneration in the retinal degeneration (rd/rd) mouse. Exp Eye Res 1997; 65:45-50. [PMID: 9237863].

71. Bowers F, Valter K, Chan S, Walsh N, Maslim J, Stone J. Effects of oxygen and bFGF on the vulnerability of photoreceptors to light damage. Invest Ophthalmol Vis Sci 2001; 42:804-15. [PMID: 11222544].

72. Tanito M, Kaidzu S, Ohira A, Anderson RE. Topography of retinal damage in light-exposed albino rats. Exp Eye Res 2008; 87:292-5. [PMID: 18586030].

73. Zhu Y, Natoli R, Valter K, Stone J. Differential gene expression in mouse retina related to regional differences in vulnerability to hyperoxia. Mol Vis 2010; 16:740-55. [PMID: 20454693].

74. Wenzel A, Grimm C, Samardzija M, Reme CE. Molecular mechanisms of light-induced photoreceptor apoptosis and neuroprotection for retinal degeneration. Prog Retin Eye Res 2005; 24:275-306. [PMID: 15610977].

75. Rozanowska M, Sarna T. Light-induced damage to the retina: role of rhodopsin chromophore revisited. Photochem Photobiol 2005; 81:1305-30. [PMID: 16120006].

76. Maeda A, Maeda T, Golczak M, Chou S, Desai A, Hoppel CL, Matsuyama S, Palczewski K. Involvement of all-trans-retinal in acute light-induced retinopathy of mice. J Biol Chem 2009; 284:15173-83. [PMID: 19304658].

77. Kranich H, Bartkowski S, Denton MJ, Krey S, Dickinson P, Duvigneau C, Gal A. Autosomal dominant "sector" retinitis pigmentosa due to a point mutation predicting an Asn-15-Ser substitution of rhodopsin. Hum Mol Genet 1993; 2:813-4. [PMID: 8353500].

78. Fujiki K, Hotta Y, Hayakawa M, Sakuma H, Shiono T, Noro M, Sakuma T, Tamai M, Hikiji K, Kawaguchi R, Hoshi A, Nakajima A, Kanai A. Point mutations of rhodopsin gene found in Japanese families with autosomal dominant retinitis pigmentosa (ADRP). Jpn J Hum Genet 1992; 37:125-32. [PMID: 1391967].

79. Heckenlively JR, Rodriguez JA, Daiger SP. Autosomal dominant sectoral retinitis pigmentosa: two families with transversion mutation in codon 23 of rhodopsin. Arch Ophthalmol 1991; 109:84-91. [PMID: 1987955].

80. Bunge S, Wedemann H, David D, Terwilliger DJ, van den Born LI, Aulehla Scholz C, Samanns C, Horn M, Ott J, Schwinger E. Molecular analysis and genetic mapping of the rhodopsin gene in families with autosomal dominant retinitis pigmentosa. Genomics 1993; 17:230-3. [PMID: 8406457].

81. Fishman GA, Stone EM, Gilbert LD, Kenna P, Sheffield VC. Ocular findings associated with a rhodopsin gene codon 58 transversion mutation in autosomal dominant retinitis pigmentosa. Arch Ophthalmol 1991; 109:1387-93. [PMID: 1929926].

82. Rivera-De la Parra D, Cabral-Macias J, Matias-Florentino M, Rodriguez-Ruiz G, Robredo V, Zenteno JC. Rhodopsin p. N78I dominant mutation causing sectorial retinitis pigmentosa in a pedigree with intrafamilial clinical heterogeneity. Gene 2013; 519:173-6. [PMID: 23402891].

83. Moore AT, Fitzke FW, Kemp CM, Arden GB, Keen TJ, Inglehearn CF, Bhattacharya SS, Bird AC. Abnormal dark adaptation kinetics in autosomal dominant sector retinitis pigmentosa due to rod opsin mutation. Br J Ophthalmol 1992; 76:465-9. [PMID: 1390527].

84. Shah SP, Wong F, Sharp DM, Vincent AL. A novel rhodopsin point mutation, proline-170-histidine, associated with sectoral retinitispigmentosa. Ophthalmic Genet 2014; 35:241-7. [PMID: 24918165].

85. Keen TJ, Inglehearn CF, Kim R, Bird AC, Bhattacharya SS, Bhattacharya S. Retinal pattern dystrophy associated with a 4 bp insertion at codon 140 in the RDS-peripherin gene. Hum Mol Genet 1994; 3:367-8. [PMID: 8004111].

86. Souied E, Gerber S, Rozet JM, Bonneau D, Dufier JL, Ghazi I, Philip N, Soubrane G, Coscas G, Munnich A. Five novel missense mutations of the rhodopsin gene in autosomal dominant retinitis pigmentosa. Hum Mol Genet 1994; 3:1433-4. [PMID: 7987331].

87. Katagiri S, Hayashi T, Akahori M, Itabashi T, Nishino J, Yoshitake K, Furuno M, Ikeo K, Okada T, Tsuneoka H, Iwata T. RHO Mutations (p.W126L and p.A346P) in Two Japanese Families with Autosomal DominantRetinitis Pigmentosa. J Ophthalmol 2014; 2014:210947-[PMID: 25485142].

88. Fujiki Y. Hotta, A. Murakami, Yoshii M, Hayakawa M, Ichikawa T, Takeda M, Akeo K, Okisaka S, Kanai A.

Missense mutation of rhodopsin gene codon 15 found in Japanese autosomal dominant retinitis pigmentosa. Jpn J Hum Genet 1995; 40:271-7. [PMID: 8527802].

89. Budu MM, Hayasaka S, Yamada T, Hayasaka Y. Rhodopsin gene codon 106 mutation (Gly-to-Arg) in a Japanese family with autosomal dominant retinitis pigmentosa Jpn J Ophthalmol 2000; 44:610-4. [PMID: 11094174].

90. Saihan Z, Stabej Ple Q, Robson AG, Rangesh N, Holder GE, Moore AT, Steel KP, Luxon LM, Bitner-Glindzicz M, Webster AR. Mutations in the USH1C gene associated with sector retinitis pigmentosa and hearing loss. Retina 2011; 31:1708-16. [PMID: 21487335].

Articles are provided courtesy of Emory University and the Zhongshan Ophthalmic Center, Sun Yat-sen University, P.R. China. The print version of this article was created on 30 December 2019. This reflects all typographical corrections and errata to the article through that date. Details of any changes may be found in the online version of the article.